

## Supporting information for

The synthesis and magnetic properties of carboxylic acid derived 1,2,4-benzotriazinyl radicals and their coordination particles

Le Qu,<sup>‡a</sup> Hanjiao Chen,<sup>‡c</sup> Chengjia Shi,<sup>a</sup> Huaqing Li,<sup>a</sup> Qi Ai,<sup>d</sup> Xuying Liu,<sup>a</sup> Cao Yang,<sup>a\*</sup> Huige Yang,<sup>a\*</sup> and Xiaoguang Hu<sup>\*ab</sup>

<sup>a</sup> School of Materials Science and Engineering, Zhengzhou University, Zhengzhou 450001, P. R. China.

<sup>b</sup> Institute of Electronic and Information Engineering of UESTC in Guangdong, 523808, P. R. China.

<sup>c</sup> Analytical & Testing Center, Sichuan University, Chengdu 610064, P. R. China.

<sup>d</sup> College of Optical and Electronic Technology, China Jiliang University, Hangzhou 310018, China.

Email address: xghu@zzu.edu.cn; yanghg@zzu.edu.cn; yc321@zzu.edu.cn.

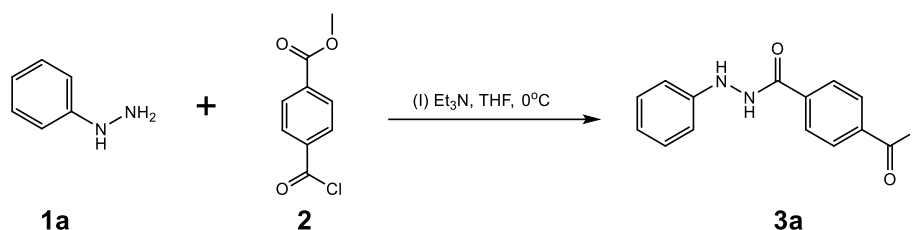
## 1. Methods and Materials

All reagents were purchased from Aladdin, Macklin and Adamas and used as received. Flash column chromatography was performed with Haiyang silica gel (200-300 mesh), All reaction mixtures and column eluents were monitored by TLC using commercial Huanghai glass plates (HSGF 254, 2.5 x 8 cm). The plates were visualized under UV radiation at 254 and 365 nm. NMR spectra were measured by a Bruker AV III HD 400 MHz. UV absorption spectra were recorded on an Agilent Cary-5000 UV-Vis-NIR spectrophotometer. High resolution mass spectra (HRMS) were measured on a ACQUITY UPLC I-CLASS (ESI). Electron spin resonance (ESR) measurements were carried out on a Bruker EMX plus X-band spectrometer with 9.8 GHz microwave frequency. SQUID measurements were carried out on a Quantum Design (MPMS3-SQUID VSM-094). Thermo gravimetric analysis (TGA) measurements were performed on Shimadzu TG-50 thermal gravimetric analyzer. Fourier transform infrared (FT-IR) spectra were measured on a Bruker Tensor-27 spectrometer. Scanning electron microscope (SEM) and energy dispersive X-ray spectrum (EDX) were performed on a Phenom ProX electron microscope energy spectrum integrated machine. HRSEM were measured on a JEOL JSM-7500F scanning electron microscope. Cyclic voltammograms (CV) were measured on a Shanghai Chenhua CHI 660E electrochemical workstation. Inductively coupled plasma mass spectrometry (ICP-MS) were measured on an Agilent 7800. X-ray Photoelectron Spectroscopy (XPS) were measured on a KRATOS AXIS Ultra DLD. Differential Scanning Calorimetry (DSC) were measured on a NETZSCH DSC214.

## 2. Preparation and characterization of radicals

### 2.1 Synthetic process

#### Synthesis of methyl 4-(2-phenylhydrazine-1-carbonyl)benzoate (**3a**)

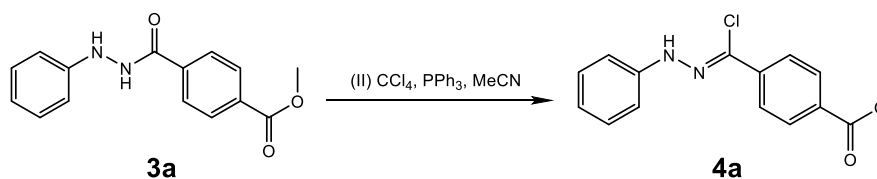


To an anhydrous tetrahydrofuran (THF) solution (40 mL) of phenylhydrazine **1a** (2.2 g, 20 mmol) and triethylamine ( $\text{Et}_3\text{N}$ ) (3.3 mL, 25 mmol) was added methyl 4-(chlorocarbonyl)benzoate **2** (4.0 g, 20 mmol) dropwise at  $0^\circ\text{C}$ . Then the mixture was stirred at room temperature for 24 h, monitored by TLC. The resulting precipitate was removed by suction filtration, followed by evaporation of THF under a reduced pressure. The yield solid was recrystallized from THF/EtOH, then dried under vacuum at  $60^\circ\text{C}$  for 24 hours to afford ethyl 4-(2-(4-(methoxycarbonyl)benzoyl)hydrazineyl)benzoate **3a** as a white polycrystal (4.3 g, 80%).

$^1\text{H}$ NMR (DMSO- $d_6$ , 400 MHz)  $\delta$  3.90 (s, 3H), 6.71-6.75 (m, 1H), 6.80 (d,  $J=8$  Hz, 2H), 7.14-7.19 (m, 2H), 7.97 (s, 1H), 8.02-8.09 (m, 4H), 10.54 (s, 1H).  $^{13}\text{C}$ NMR (DMSO- $d_6$ , 100 MHz)  $\delta$  52.89, 112.80, 119.21, 128.21, 129.23, 129.74, 132.60, 137.63, 149.73, 166.04, 166.13.

HRMS( $\text{ESI}^+$ ): calcd. for  $\text{C}_{15}\text{H}_{14}\text{N}_2\text{O}_3$  270.1004, found  $[\text{M}+\text{Na}]^+$  293.1129.

#### Synthesis of Methyl 4-[chloro(2-phenylhydrazinylidene)methyl]benzoate (**4a**)



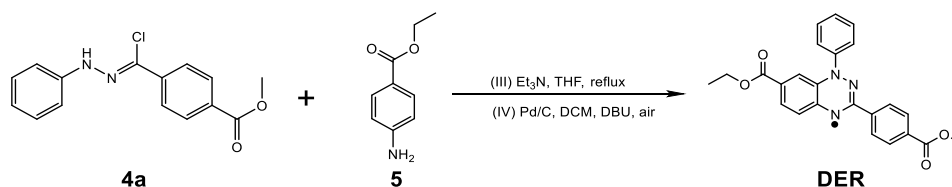
To an acetonitrile (MeCN) (50 mL) solution of compound **3a** (1.4 g, 5 mmol) was added triphenylphosphine (1.6 g, 5 mmol) and carbon tetrachloride (0.6 mL, 5 mmol). Then

the reaction mixture was stirred at room temperature for 16 h, monitored by TLC. Solvent was removed under reduced pressure and the residue was purified by column chromatography (silica gel, petroleum ether/ethyl acetate, V/V = 30: 1) to give methyl 4-[chloro[2-(4-ethylbenzoate)hydrazinylidene]methyl]benzoate **4a** as a yellow green solid (1.1 g, 75 %).

$^1\text{H}$ NMR ( $\text{CDCl}_3$ , 400 MHz)  $\delta$  3.97 (s, 3H), 6.98-7.03 (m, 1H), 7.23 (d,  $J=8$  Hz, 2H), 7.34-7.38 (m, 2H), 8.01 (d,  $J=8$  Hz, 2H), 8.09 (d,  $J=8$  Hz, 2H), 8.19 (s, 1H).  $^{13}\text{C}$ NMR ( $\text{CDCl}_3$ , 100 MHz)  $\delta$  52.24, 113.64, 121.70, 123.54, 126.08, 129.46, 129.67, 130.27, 138.45, 142.86, 166.59.

HRMS( $\text{ESI}^+$ ): calcd. for  $\text{C}_{15}\text{H}_{13}\text{N}_2\text{O}_3\text{Cl}$  288.0666, found  $[\text{M}-\text{Cl}]^+$  253.10375.

### Synthesis of DER

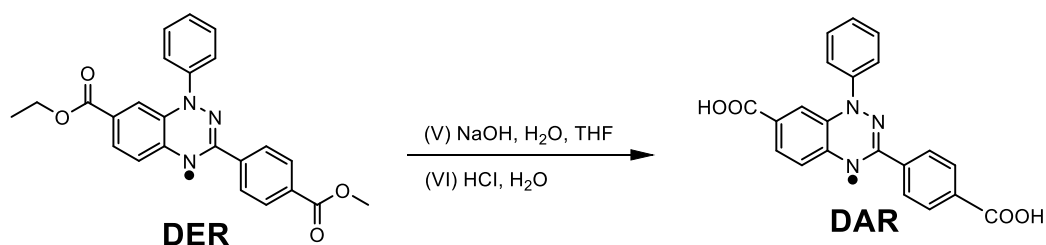


To an anhydrous THF solution (20 mL) of **4a** (1.0 g, 3.5 mmol) and **5** (0.6 g, 3.5 mmol) was added  $\text{Et}_3\text{N}$  (1.0 mL) at room temperature. Then the mixture was heated to reflux for 24 h, monitored by TLC. The resulting mixture was cooled to room temperature and the precipitate was removed by suction filtration, followed by evaporation of THF under a reduced pressure. The residue was purified by column chromatography (silica gel, petroleum ether/ethyl acetate, V/V = 30: 1) to yield the intermediate as yellow oil. Then the residue was dissolved in dry DCM (10 mL), and treated with 1,8-diazabicyclo [5.4.0] undec-7-ene (DBU) (1 mL) and 10 wt% Pd/C powder (20 mg). The reaction mixture was stirred in open air for 24 h, upon filtration the resulting filtrate was evaporated to yield black crude solid. This solid was purified by column chromatography (silica gel, petroleum ether/ethyl acetate, V/V = 20: 1) and recrystallized from DCM/petroleum ether to give **DER** as a brown solid (1.0 g, 70%).

$^1\text{H}$ NMR ( $\text{DMSO}-d_6$ , reduced with  $\sim 1$  equivalent ascorbic acid to form the triazine)  $\delta$  9.29 (s, 1H), 8.05 (d,  $J=8$  Hz, 2H), 7.97 (d,  $J=8$  Hz, 2H), 7.46-7.47 (m, 4H), 7.40 (d,  $J=8$  Hz, 1H), 7.19-7.23 (m, 1H), 6.83 (s, 1H), 6.79 (d,  $J=8$  Hz, 1H).

HRMS(ESI<sup>+</sup>): calcd. for C<sub>24</sub>H<sub>20</sub>N<sub>3</sub>O<sub>4</sub> 414.1454, found 414.1772. Melting range: 256-258°C.

### Synthesis of DAR

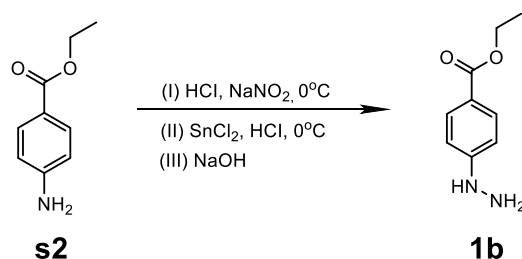


To a stirred mixture of **DER** (60 mg, 0.16 mmol) in THF/H<sub>2</sub>O (20 mL/10 mL) was added 2 M NaOH (0.8 mL), then the reaction mixture was heated to reflux for 5 h. After cooling to room temperature, THF was removed under a reduced pressure. pH value of the aqueous solution was adjusted to 5-6 with 2M HCl. The precipitate was collected by centrifugation and washed with deionized water for three times, then dried under vacuum at 60°C for 24 hours to afford **DAR** as a black solid (50 mg, 83%).

<sup>1</sup>HNMR (DMSO-*d*<sub>6</sub>, reduced with ~1 equivalent ascorbic acid to form the triazine)  $\delta$  9.24 (s, 1H), 8.02 (d, *J* = 8 Hz, 2H), 7.95 (d, *J* = 8 Hz, 2H), 7.46-7.47 (m, 4H), 7.38 (d, *J* = 8 Hz, 1H), 7.18-7.22 (m, 1H), 6.84 (s, 1H), 6.78 (d, *J* = 8 Hz, 1H).

HRMS(ESI<sup>+</sup>): calcd. for C<sub>21</sub>H<sub>14</sub>N<sub>3</sub>O<sub>4</sub> 372.0984, found 372.1050. Melting range: 365-370°C.

### Synthesis of ethyl 4-hydrazineylbenzoate (**1b**)



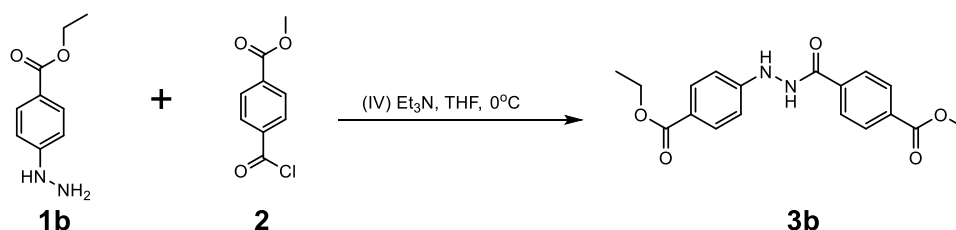
To a stirred concentrated HCl (60 mL) solution of ethyl 4-aminobenzoate **s2** (11.0 g, 66 mmol) was added a freshly prepared solution of NaNO<sub>2</sub> (4.6 g, 66 mmol) in water (30 mL) dropwise over 10 minutes at 0°C. After stirring at room temperature for 90 minutes, the reaction mixture was added a solution of SnCl<sub>2</sub>·2H<sub>2</sub>O (44.7 g, 198 mmol) in

concentrated HCl (30 mL) dropwise at 0°C, then stirred at room temperature for 2 hours. The formed precipitate was collected by filtration and then dissolved in water (300 mL). Then the pH of the solution was adjusted to 8-9 by 2M NaOH, the formed precipitate was filtered and dried under vacuum at 60°C for 24 hours to afford ethyl 4-hydrazineylbenzoate **1b** as a light yellow solid (9.75 g, 82%).

<sup>1</sup>HNMR (CDCl<sub>3</sub>, 400 MHz) δ 1.37-1.42 (m, 3H), 3.67 (s, 2H), 4.32-4.38 (m, 2H), 5.55 (s, 1H), 6.82 (d, *J* = 8.0 Hz, 2H), 7.95 (d, *J* = 8.0 Hz, 2H). <sup>13</sup>CNMR (CDCl<sub>3</sub>, 100 MHz) δ 14.4, 60.3, 110.6, 120.7, 131.4, 154.6, 166.7.

HRMS(ESI<sup>+</sup>): calcd. for C<sub>9</sub>H<sub>13</sub>N<sub>2</sub>O<sub>2</sub> 181.0977, found [M+H]<sup>+</sup> 181.1061.

### Synthesis of ethyl 4-(2-(4-(methoxycarbonyl)benzoyl)hydrazineyl)benzoate (**3b**)

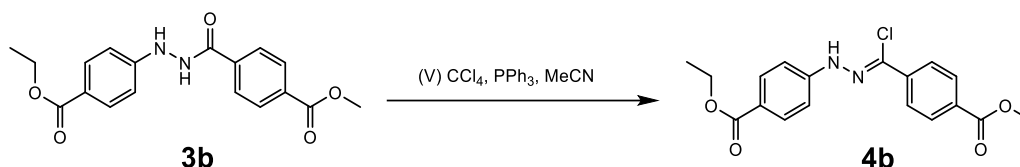


To an anhydrous THF solution (50 mL) of **1b** (1.8 g, 10 mmol) and Et<sub>3</sub>N (2.7 mL, 20 mmol) was added methyl 4-(chlorocarbonyl)benzoate **2** (1.99 g, 10 mmol) dropwise at 0°C. Then the mixture was stirred at room temperature for 24 h, monitored by TLC. The resulting precipitate was removed by suction filtration, followed by evaporation of THF under a reduced pressure. The yield solid was recrystallized from THF/EtOH, then dried under vacuum at 60°C for 24 hours to afford ethyl 4-(2-(4-(methoxycarbonyl)benzoyl)hydrazineyl)benzoate **3b** as a white solid (2.8 g, 82%).

<sup>1</sup>HNMR (DMSO-d<sub>6</sub>, 400 MHz) δ 1.25-1.31 (m, 3H), 4.20-4.27 (m, 2H), 5.90 (s, 3H), 6.81 (d, *J* = 8.0 Hz, 2H), 7.78 (d, *J* = 8.0 Hz, 2H), 8.03-8.11 (m, 4H), 8.71 (s, 1H), 10.68 (s, 1H). <sup>13</sup>CNMR (DMSO-d<sub>6</sub>, 100 MHz) δ 14.8, 52.9, 60.3, 111.6, 119.8, 128.3, 129.8, 131.2, 132.8, 137.2, 153.7, 166.0, 166.1, 166.1.

HRMS (ESI<sup>+</sup>): calcd. for C<sub>18</sub>H<sub>18</sub>N<sub>2</sub>O<sub>5</sub> 342.1216, found [M+Na]<sup>+</sup> 365.1414.

### Synthesis of methyl 4-[chloro[2-(4-ethylbenzoate)hydrazinylidene]methyl]benzoate (**4b**)

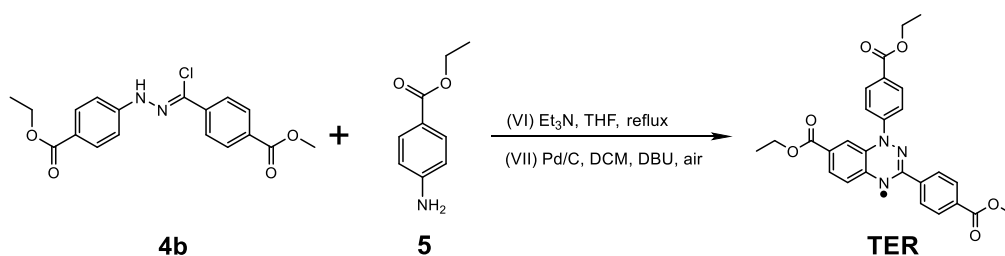


To an acetonitrile (MeCN) (80 mL) solution of compound **3b** (1.0 g, 3 mmol) was added triphenylphosphine (1.1 g, 4 mmol) and carbon tetrachloride (0.4 mL, 4 mmol). Then the reaction mixture was stirred at room temperature for 16 h, monitored by TLC. Solvent was removed under reduced pressure and the residue was purified by column chromatography (silica gel, petroleum ether/ethyl acetate, V/V = 10: 1) to give methyl 4-[chloro[2-(4-ethylbenzoate)hydrazinylidene]methyl]benzoate **4b** as a yellow green solid (1.0 g, 68 %).

$^1\text{H}$ NMR ( $\text{CDCl}_3$ , 400 MHz)  $\delta$  1.39-1.45 (m, 3H), 3.98 (s, 3H), 4.35-4.43 (m, 2H), 7.24 (d,  $J = 8\text{ Hz}$ , 2H), 8.00-8.08 (m, 4H), 8.11 (d,  $J = 8\text{ Hz}$ , 2H), 8.37 (s, 1H).  $^{13}\text{C}$ NMR ( $\text{DMSO-d}_6$ , 100 MHz)  $\delta$  14.76, 52.7, 60.6, 113.8, 122.3, 124.0, 126.9, 130.0, 130.5, 131.2, 138.5, 148.1, 165.9, 166.1.

HRMS ( $\text{ESI}^+$ ): calcd. for  $\text{C}_{18}\text{H}_{18}\text{ClN}_2\text{O}_4$  361.0955, found  $[\text{M}+\text{H}]^+$  361.1003.

### Synthesis of TER



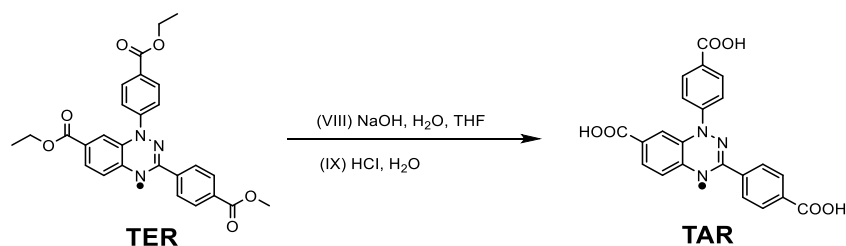
To an anhydrous THF solution (20 mL) of **4b** (0.7 g, 1.8 mmol) and **5** (0.3 g, 1.8 mmol) was added  $\text{Et}_3\text{N}$  (0.4 mL) at room temperature. Then the mixture was heated to reflux for 24 h, monitored by TLC. The resulting mixture was cooled to room temperature and the precipitate was removed by suction filtration, followed by evaporation of THF under a reduced pressure. The residue was purified by column chromatography (silica gel, petroleum ether/ethyl acetate, V/V = 15: 1) to yield the intermediate as light yellow solid. Then the residue was dissolved in dry DCM (10 mL), and treated with 1,8-diazabicyclo [5.4.0] undec-7-ene (DBU) (1 mL) and 10 wt% Pd/C powder (20 mg).

The reaction mixture was stirred in open air for 24 h, upon filtration the resulting filtrate was evaporated to yield black crude solid. This residue was purified by column chromatography (silica gel, petroleum ether/ethyl acetate, V/V = 20: 1) and recrystallized from DCM/petroleum ether to give **TER** as a brown solid (0.6 g, 67%).

<sup>1</sup>HNMR (DMSO-*d*<sub>6</sub>, reduced with ~1 equivalent ascorbic acid to form the triazine) δ 9.63 (s, 1H), 8.08 (d, *J* = 8 Hz, 2H), 8.03 (d, *J* = 8 Hz, 2H), 7.98 (d, *J* = 8 Hz, 2H), 7.61 (d, *J* = 8 Hz, 2H), 7.53 (d, *J* = 8 Hz, 1H), 7.31(s, 1H), 6.93 (d, *J* = 8 Hz, 1H).

HRMS(ESI<sup>+</sup>): calcd.for C<sub>27</sub>H<sub>24</sub>N<sub>3</sub>O<sub>6</sub> 486.1665, found 486.2016. Melting range: 227-229°C.

### Synthesis of **TAR**



To a stirred mixture of **TER** (0.3 g, 0.5mmol) in THF/H<sub>2</sub>O (25 mL/10 mL) was added 2 M NaOH (3 mL), then the reaction mixture was heated to reflux for 5 h. After cooling to room temperature, THF was removed under a reduced pressure. pH value of the aqueous solution was adjusted to 5-6 with 2M HCl. The precipitate was collected by centrifugation and washed with deionized water for three times, then dried under vacuum at 60°C for 24 hours to afford **TAR** as a black solid (0.20 g, 97%).

<sup>1</sup>HNMR (DMSO-*d*<sub>6</sub>, reduced with ~1 equivalent ascorbic acid to form the triazine) δ 9.54 (s, 1H), 8.06 (d, *J* = 8 Hz, 2H), 8.01 (d, *J* = 8 Hz, 2H), 7.96 (d, *J* = 8 Hz, 2H), 7.59 (d, *J* = 8 Hz, 2H), 7.50 (d, *J* = 8 Hz, 1H), 7.28 (s, 1H), 6.91 (d, *J* = 8 Hz, 1H).

HRMS(ESI<sup>+</sup>): calcd.for C<sub>22</sub>H<sub>14</sub>N<sub>3</sub>O<sub>6</sub> 416.0885, found 416.0574. Melting range: 360-365°C.



## 2.2 NMR and Mass spectra

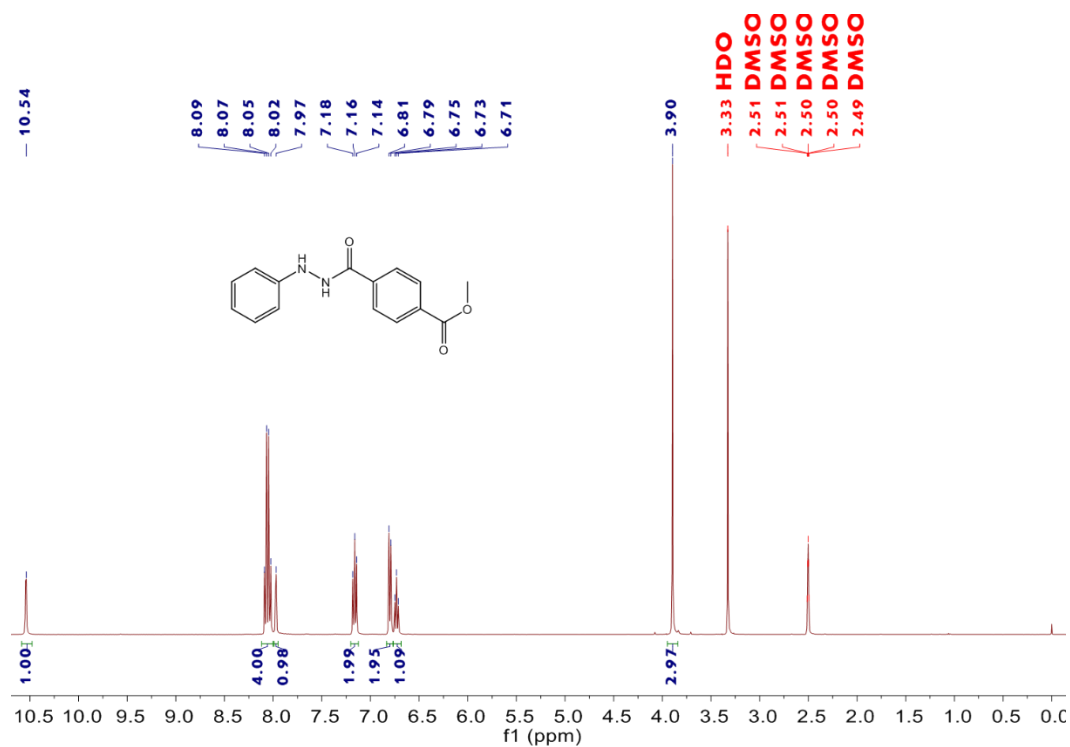


Figure S1.  $^1\text{H}$ NMR spectrum of **3a** in  $\text{DMSO-d}_6$ .

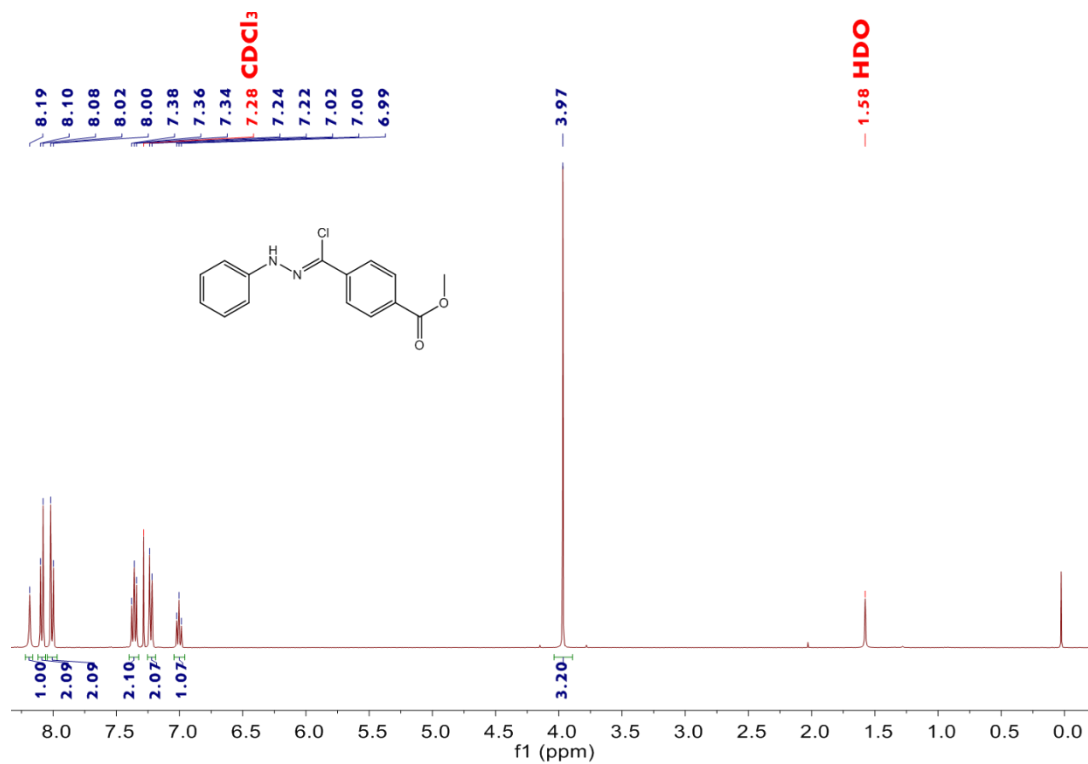
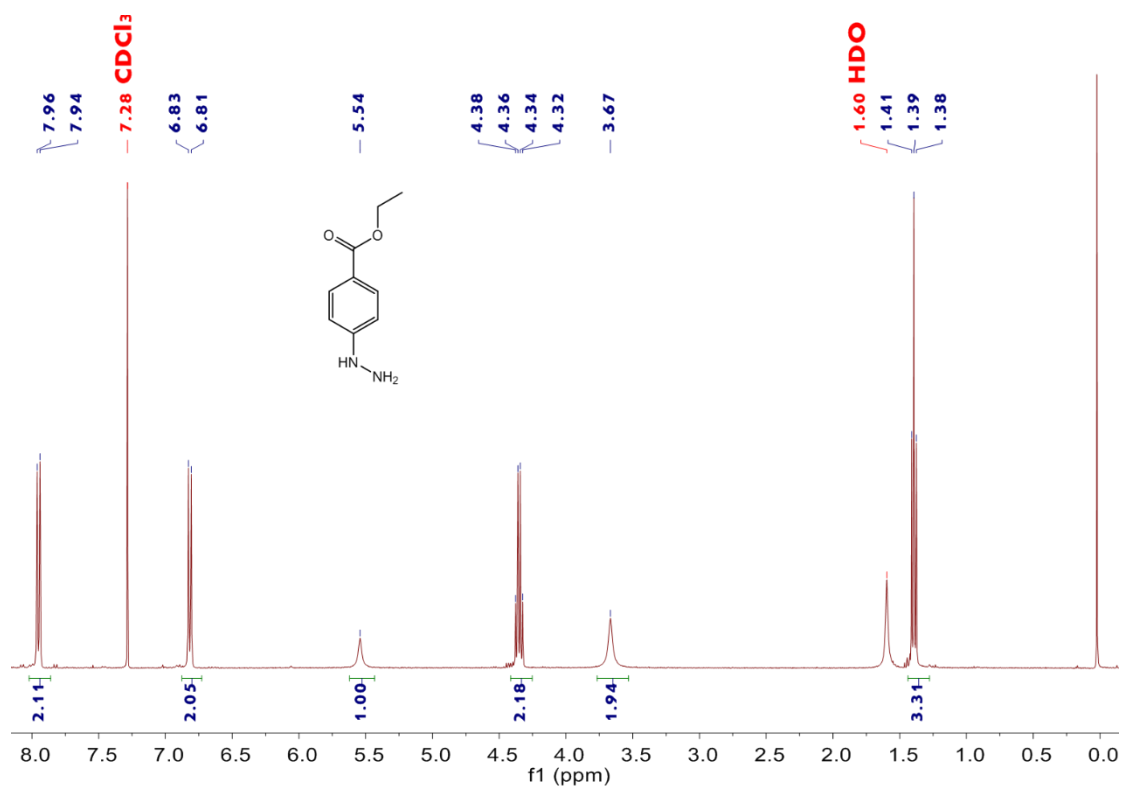
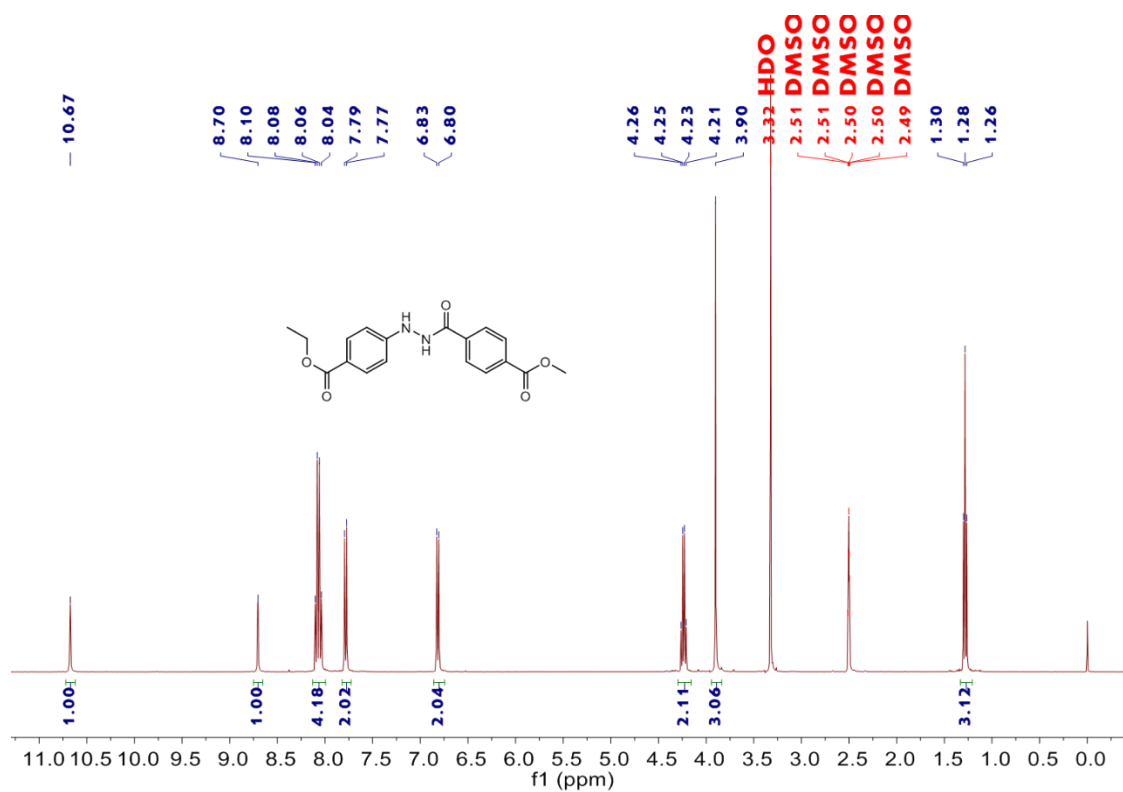


Figure S2.  $^1\text{H}$ NMR spectrum of **4a** in  $\text{CDCl}_3$ .



**Figure S3.** <sup>1</sup>H NMR spectrum of **1b** in CDCl<sub>3</sub>.



**Figure S4.** <sup>1</sup>H NMR spectrum of **3b** in DMSO-d<sub>6</sub>.

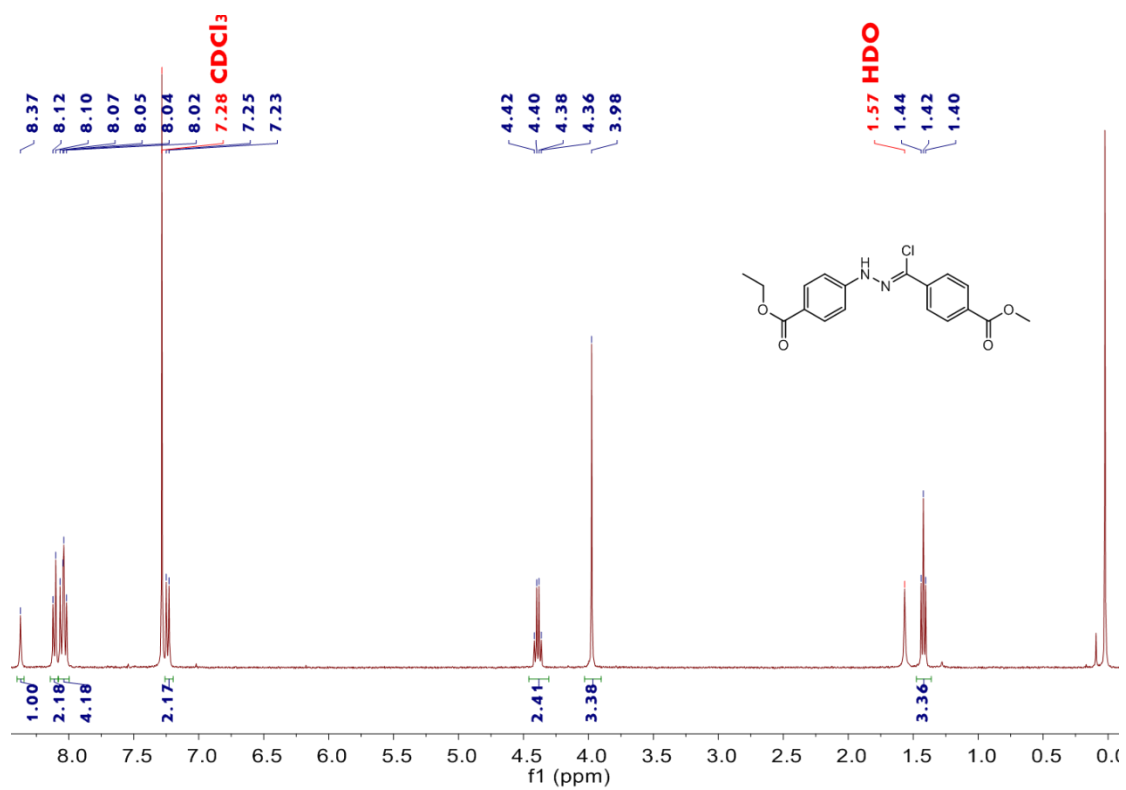


**Figure S5.**  $^1\text{H}$ NMR spectrum of **4b** in  $\text{CDCl}_3$ .

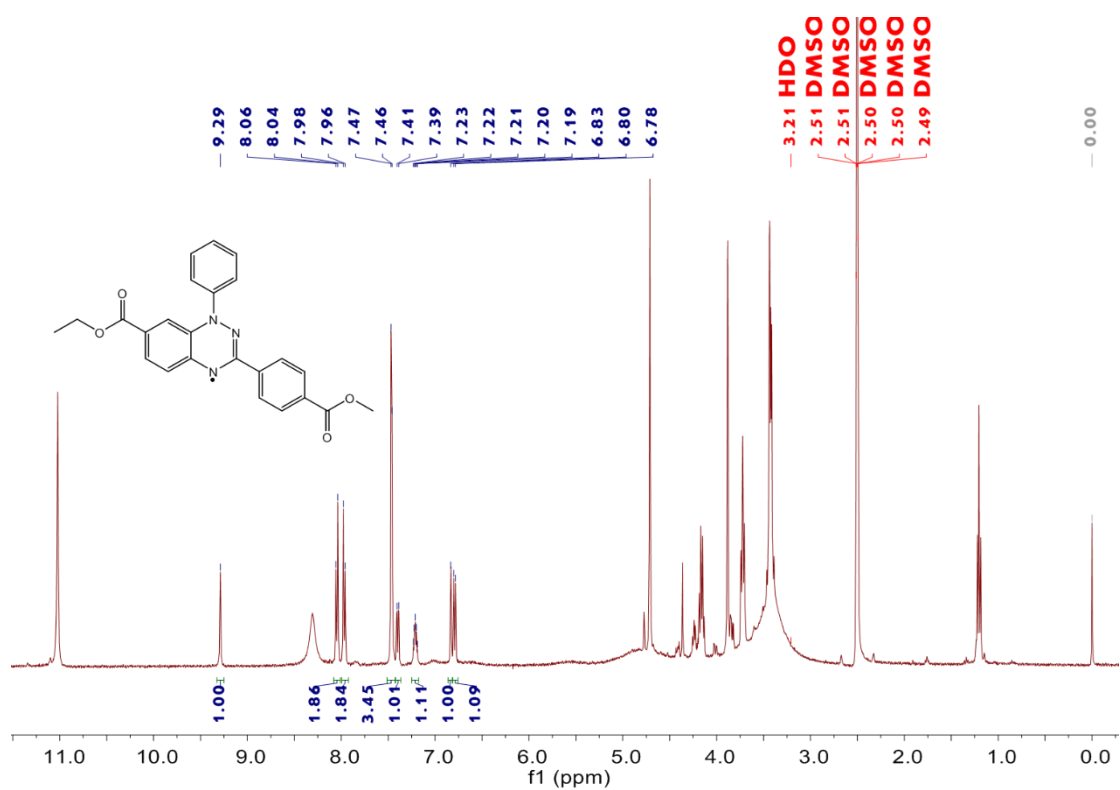


**Figure S6.**  $^1\text{H}$ NMR spectrum of **DER** in  $\text{DMSO-d}_6$ .

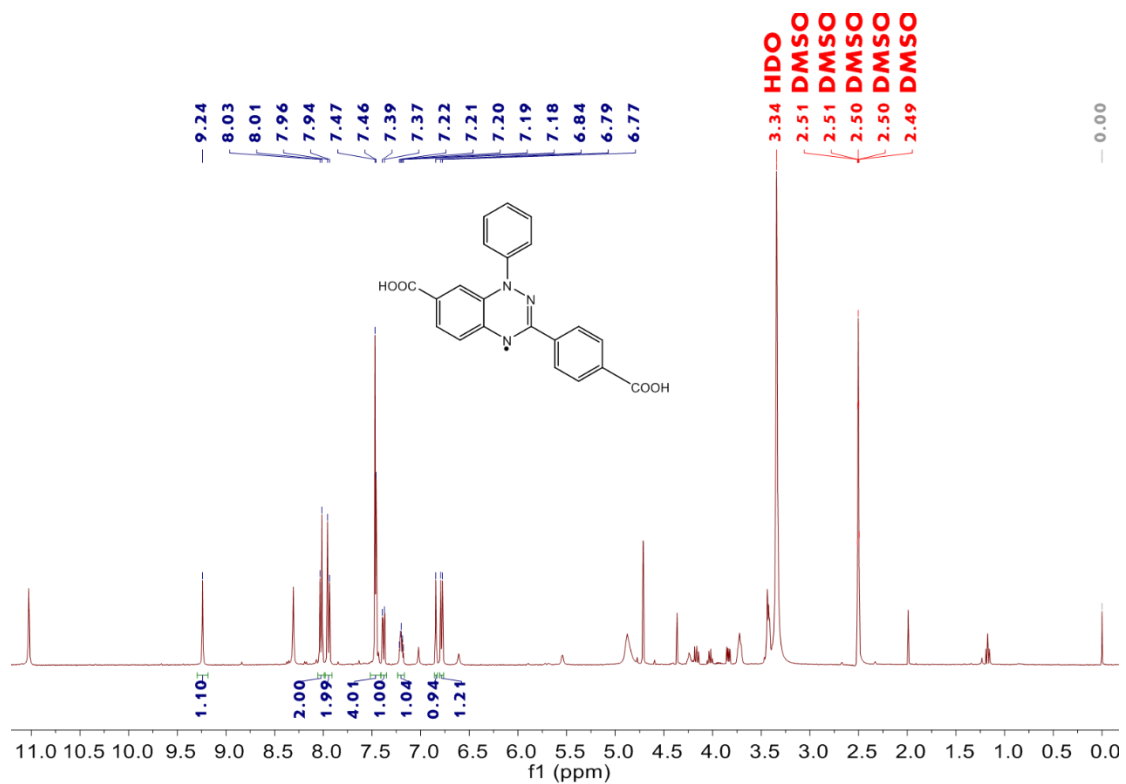


Figure S7. <sup>1</sup>H NMR spectrum of DAR in DMSO-d<sub>6</sub>.

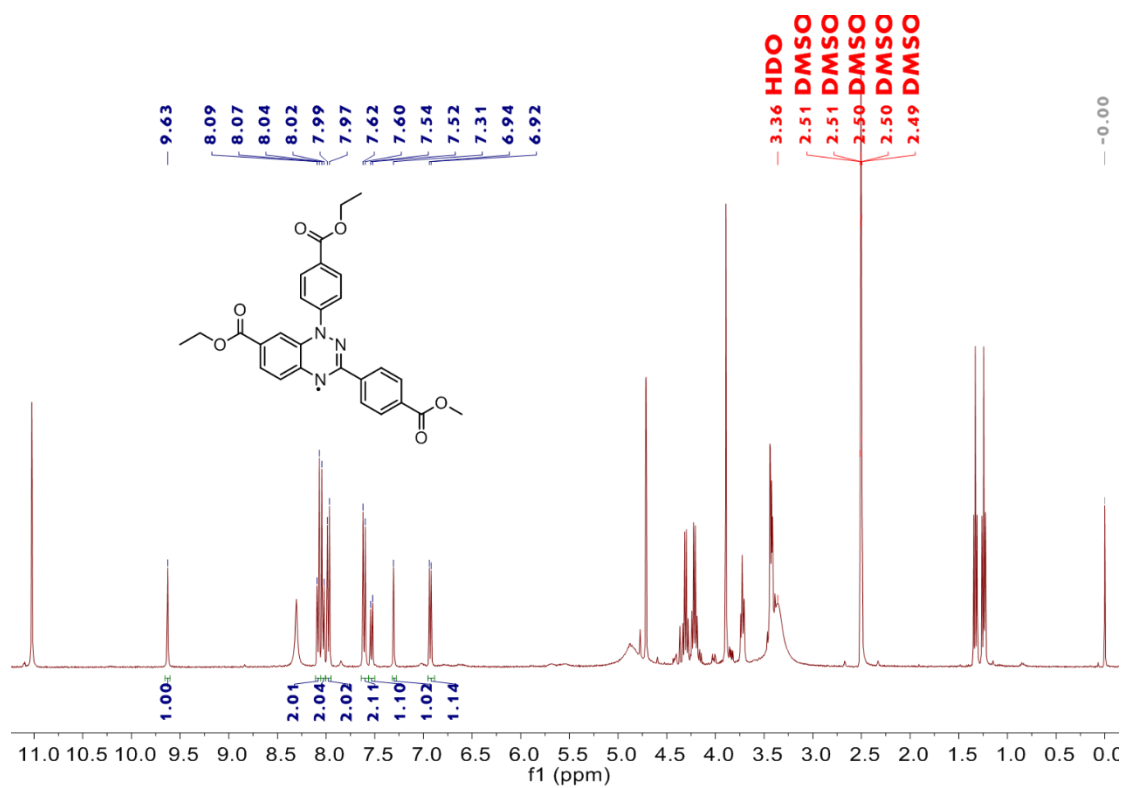


Figure S8. <sup>1</sup>H NMR spectrum of TER in DMSO-d<sub>6</sub>.

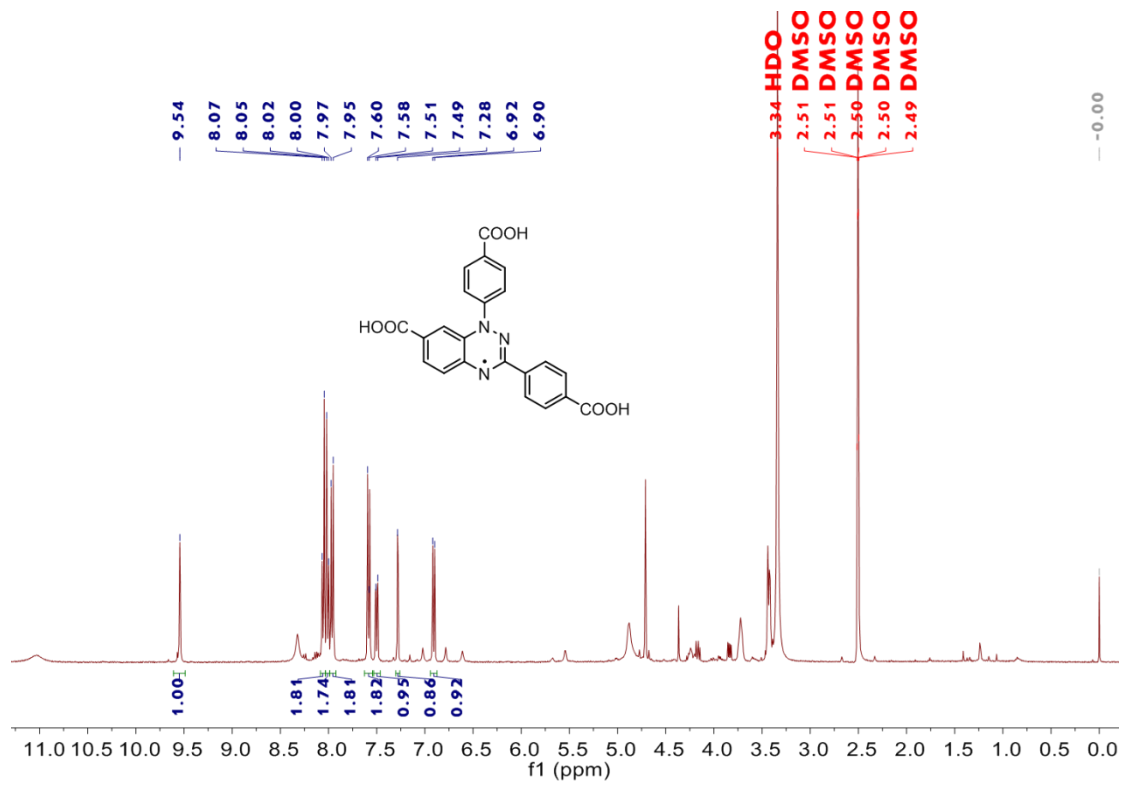


Figure S9. <sup>1</sup>H NMR spectrum of TAR in DMSO-d<sub>6</sub>.

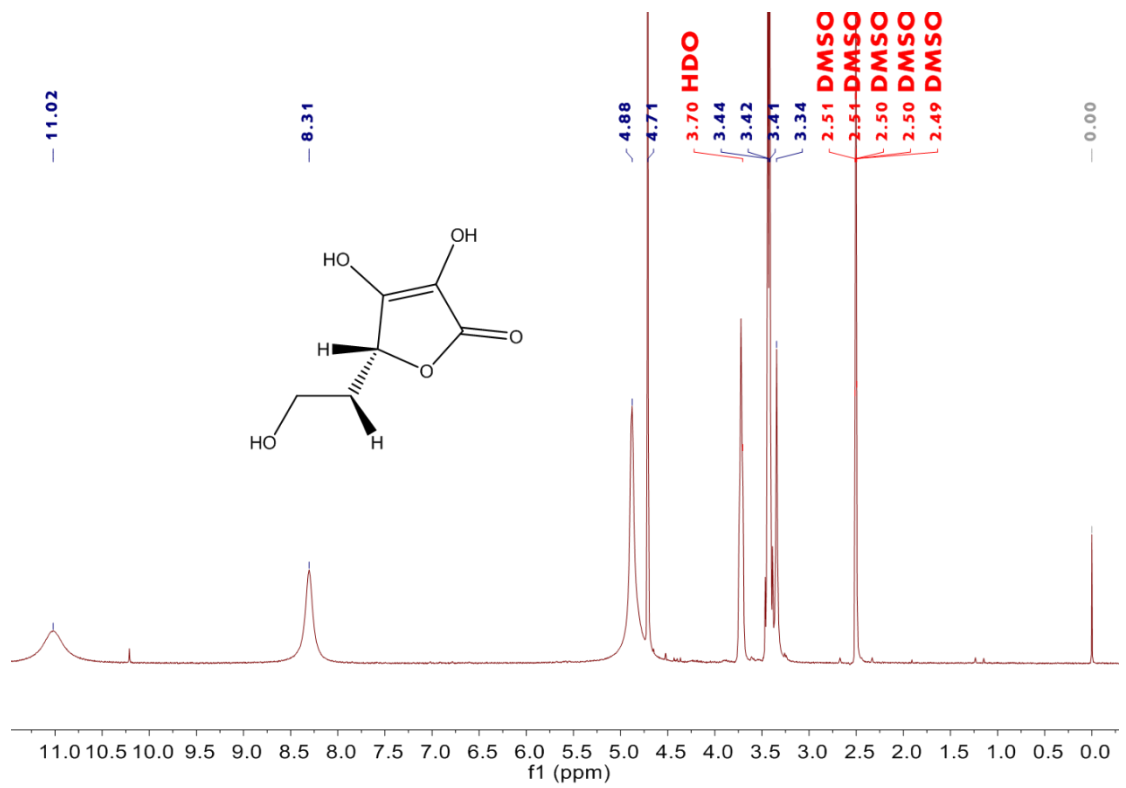


Figure S10. <sup>1</sup>H NMR spectrum of Ascorbic Acid in DMSO-d<sub>6</sub>.

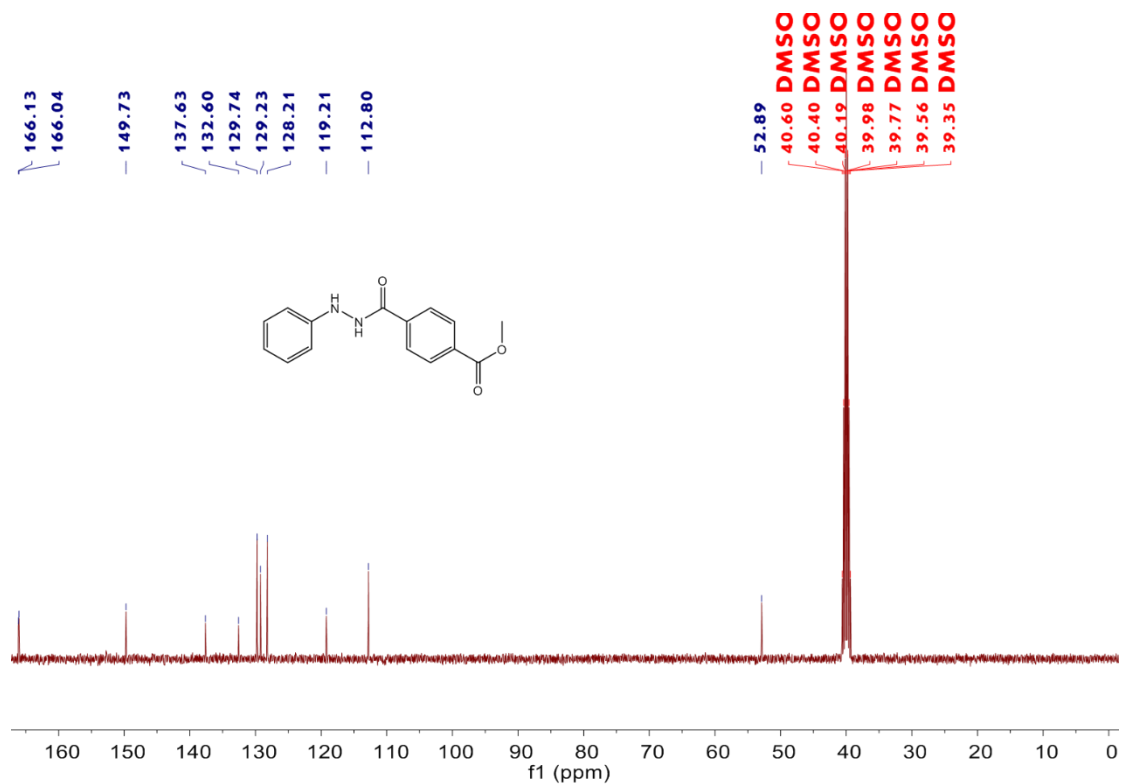


Figure S11.  $^{13}\text{C}$ NMR spectrum of **3a** in  $\text{DMSO-d}_6$ .

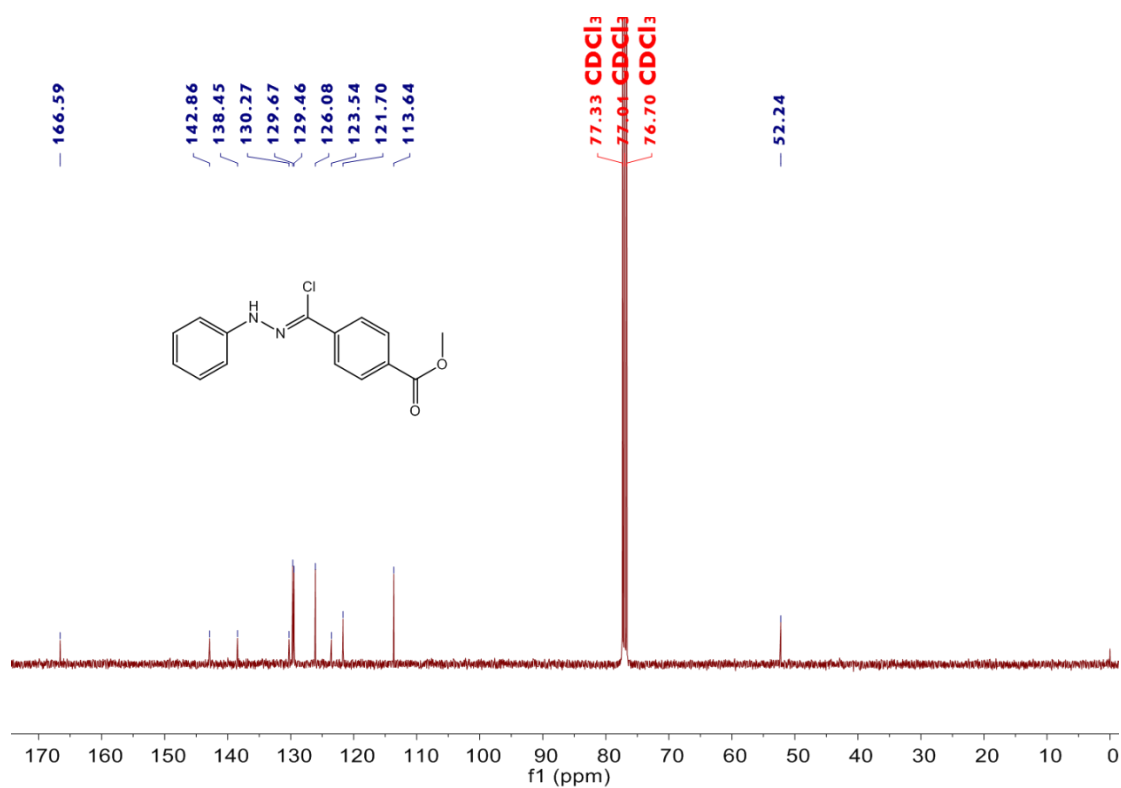


Figure S12.  $^{13}\text{C}$ NMR spectrum of **4a** in  $\text{CDCl}_3$ .

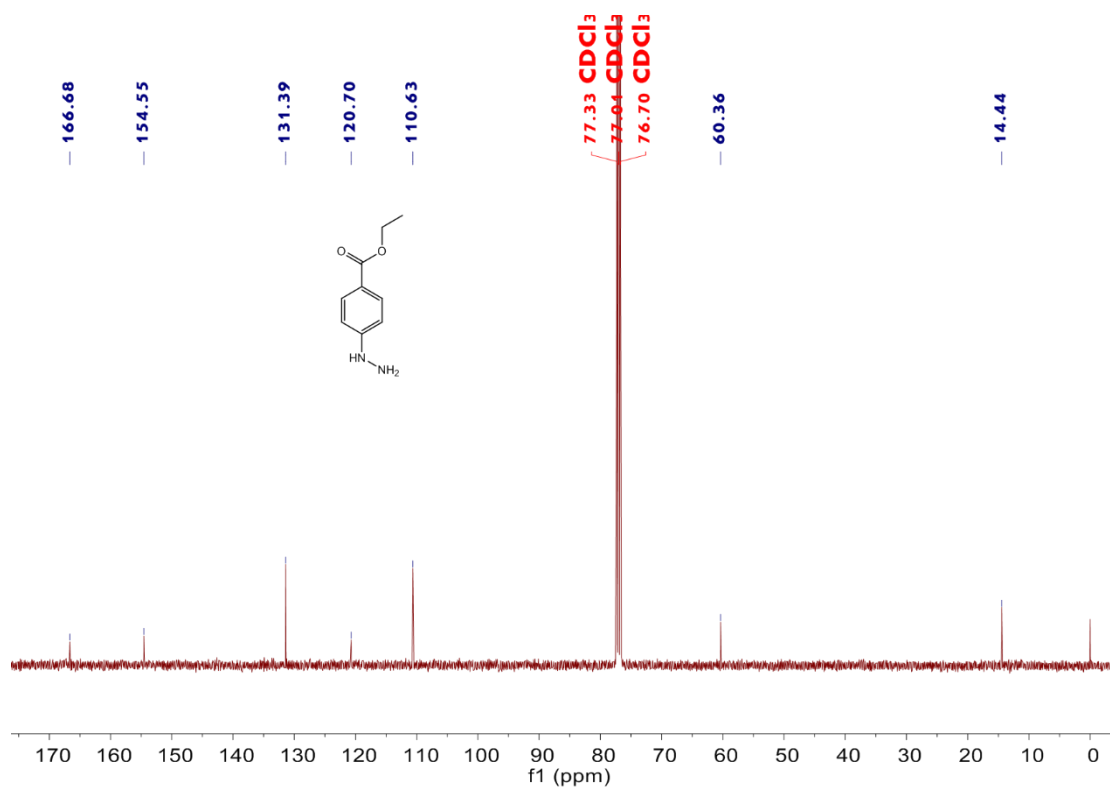


Figure S13.  $^{13}\text{C}$ NMR spectrum of **1b** in  $\text{CDCl}_3$ .

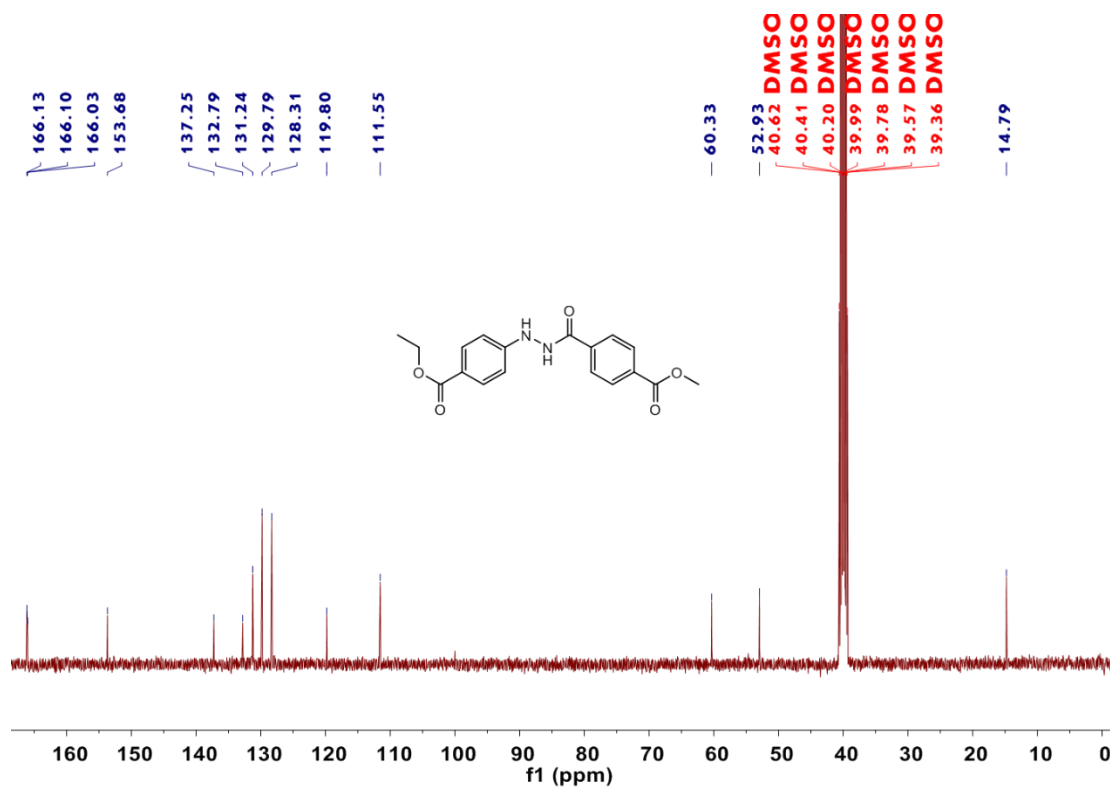


Figure S14.  $^{13}\text{C}$ NMR spectrum of **3b** in  $\text{DMSO}-d_6$ .

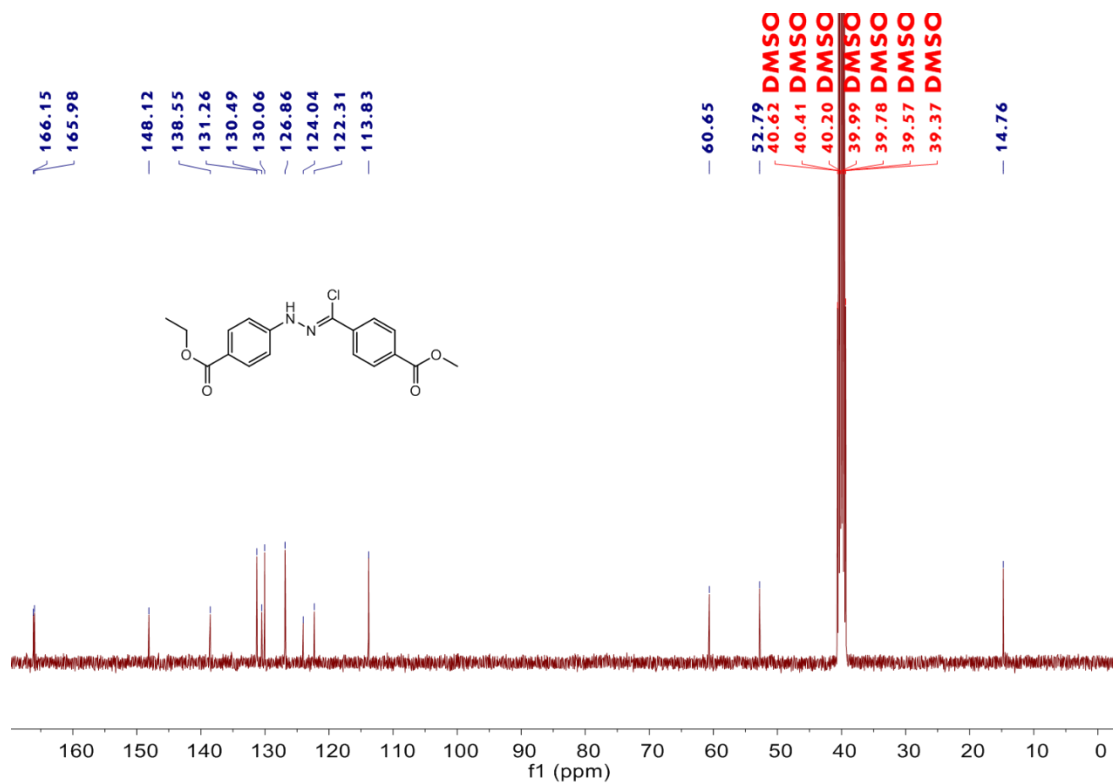
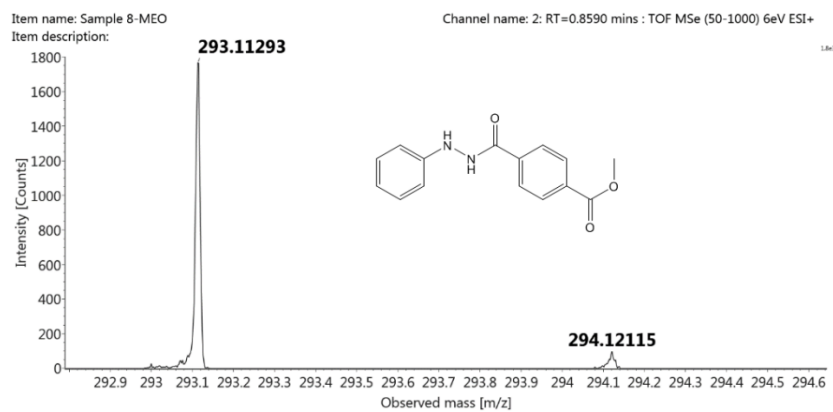
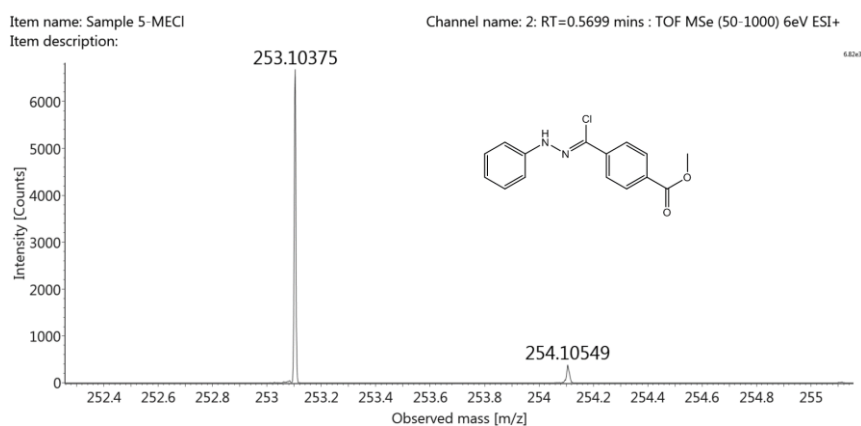


Figure S15.  $^{13}\text{C}$ NMR spectrum of **4b** in  $\text{DMSO-d}_6$ .

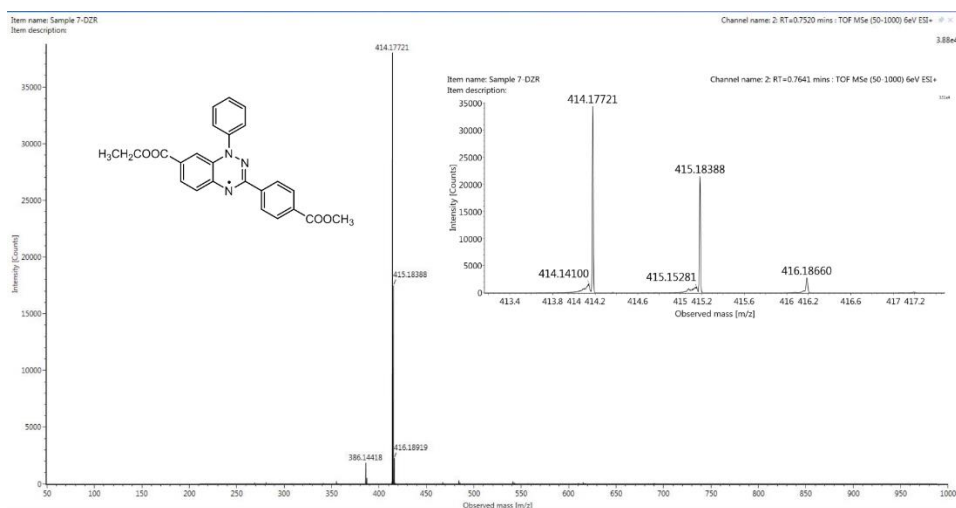




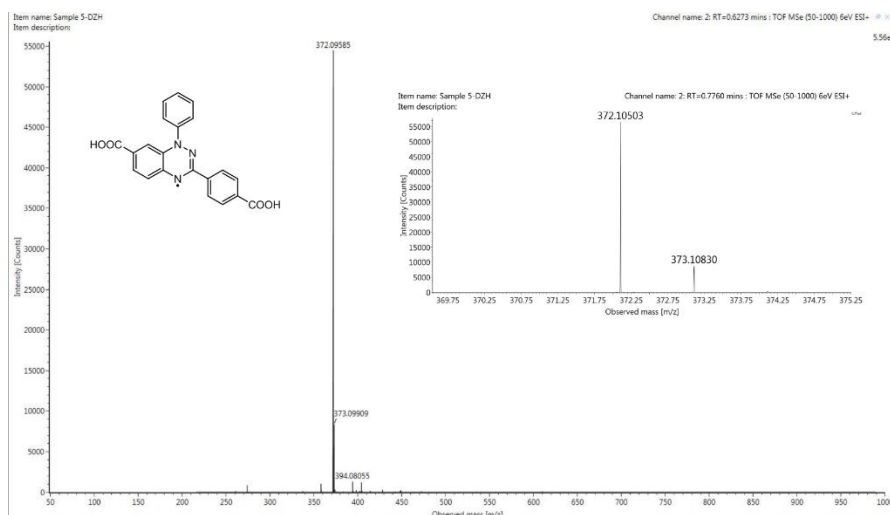
**Figure S16.** HRMS (ESI) spectrum of **3a**.



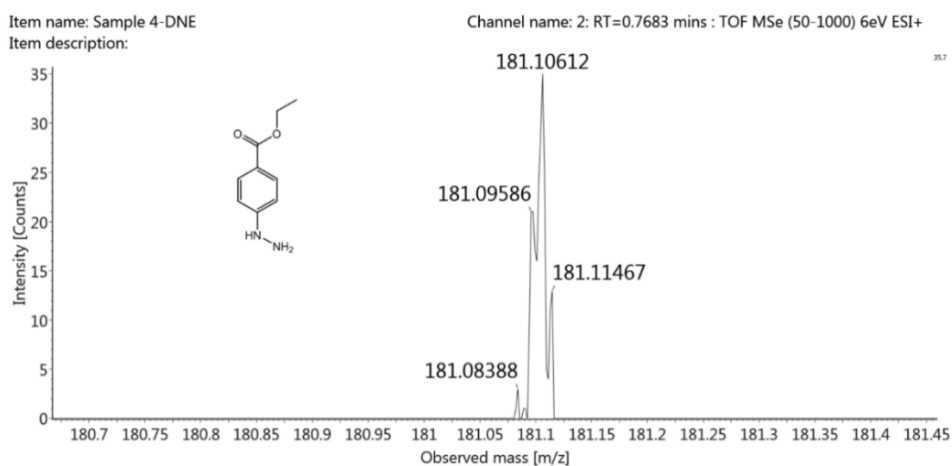
**Figure S17.** HRMS (ESI) spectrum of **4a**.



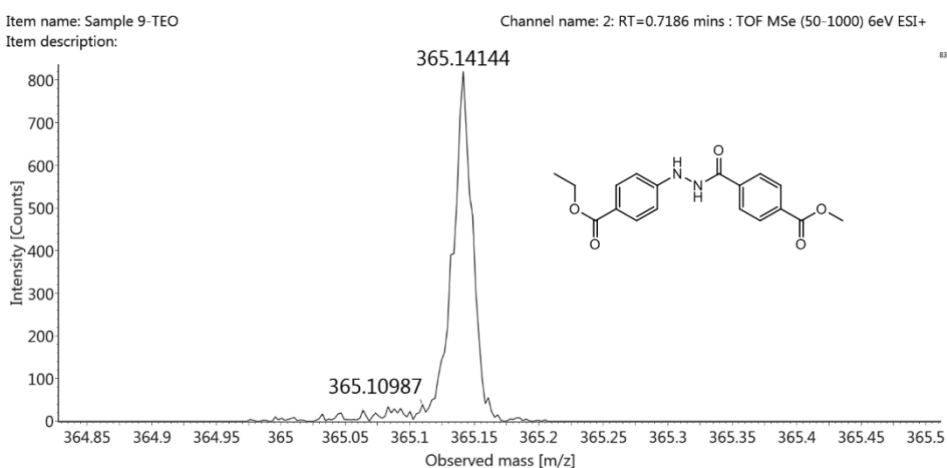
**Figure S18.** HRMS (ESI) spectrum of **DER**.



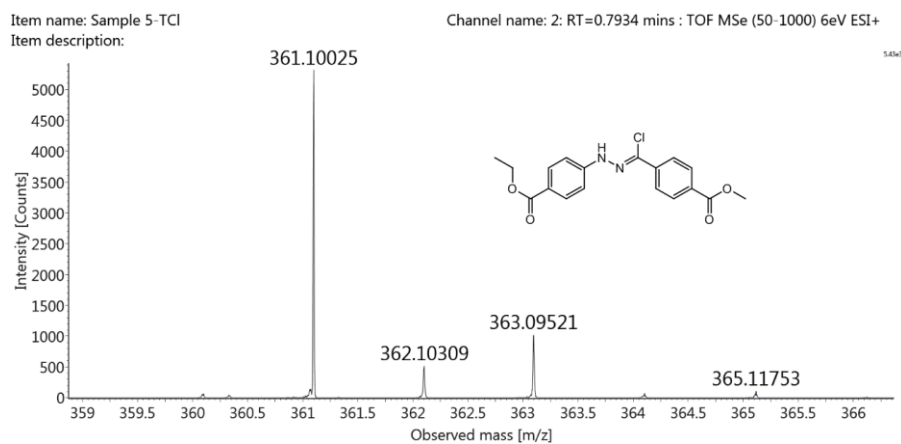
**Figure S19.** HRMS (ESI) spectrum of **DAR**.



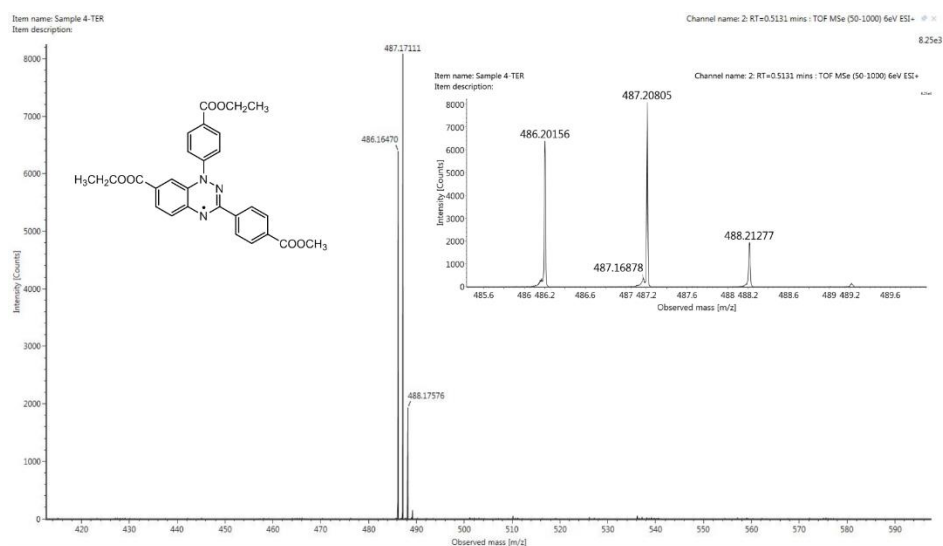
**Figure S20.** HRMS (ESI) spectrum of **1b**.



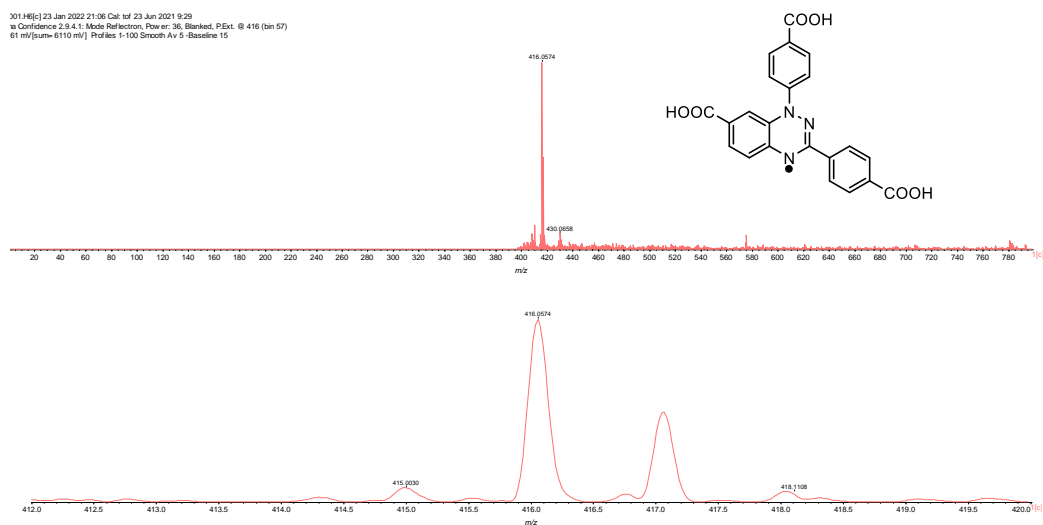
**Figure S21.** HRMS (ESI) spectrum of **3b**.



**Figure S22.** HRMS (ESI) spectrum of **4b**.



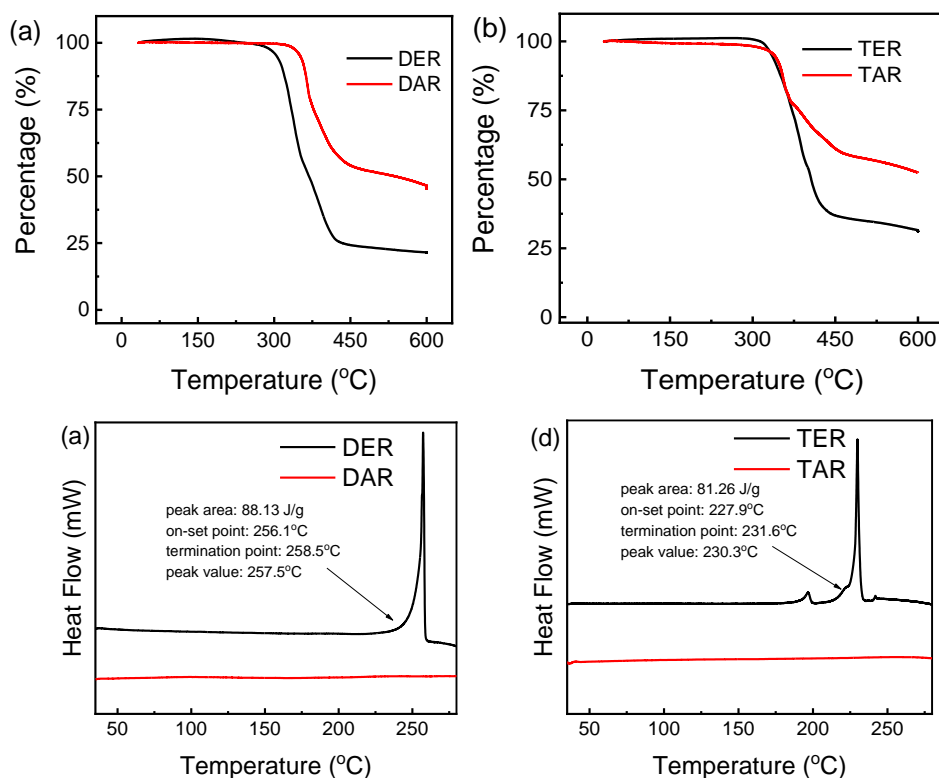
**Figure S23.** HRMS (ESI) spectrum of **TER**.



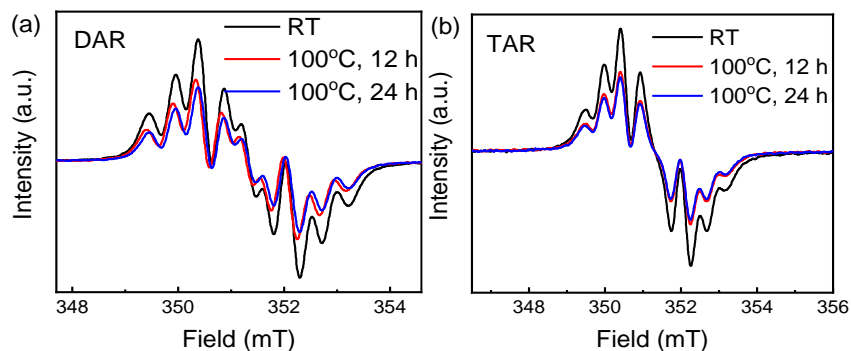
**Figure S24.** HRMS (ESI) spectrum of **TAR**.

## 2.3 Thermostability measurement

All solid samples were dried under vacuum at 60 °C for 8 h before TGA measurements. TGA curves revealed no obvious weight loss between 30 and 300 °C, indicating that all radicals are stable up to ~300 °C.



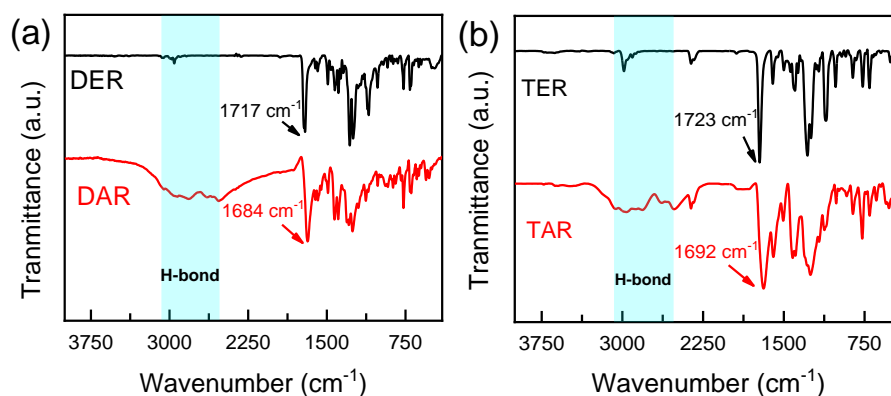
**Figure S25.** TGA diagrams of (a) **DER**, **DAR** and (b) **TER**, **TAR** under N<sub>2</sub>; heating rate = 10 °C/min. DSC spectra of (c) **DER**, **DAR** and (d) **TER**, **TAR**.



**Figure S26.** ESR spectra of **DAR** (a) and **TAR** (b) in DMF at room temperature (black line), 100 °C maintained for 12 (red line) and 24 hours (blue line).

## 2.4 Fourier transform infrared (FT-IR) spectra

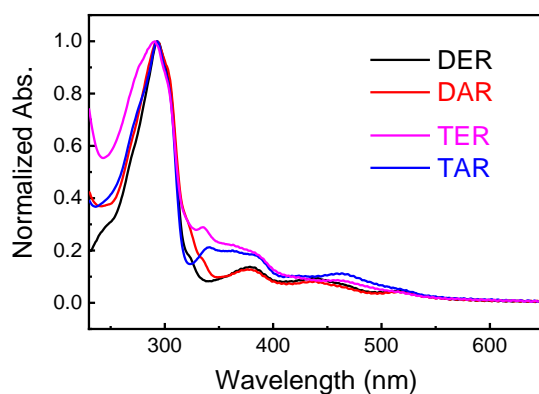
Before FT-IR measurements, the samples were dried in vacuum at 60°C for 24 hours, and the potassium bromide (KBr) was dried in oven at 120°C for 4 hours. The absence of typical N-H stretching vibration absorption above 3100 cm<sup>-1</sup> indicates that intermediates are fully converted into radicals. The C=O stretching vibration bands shifted from ~1720 cm<sup>-1</sup> to ~1690 cm<sup>-1</sup>, meanwhile broad peak appeared at 2500-3000 cm<sup>-1</sup> caused by hydroxyl association of carboxylic acid groups. These results proved that ester groups were hydrolyzed to carboxylic acid groups.



**Figure S27.** FT-IR spectra of **DER, DAR** (a) and **TER, TAR** (b).

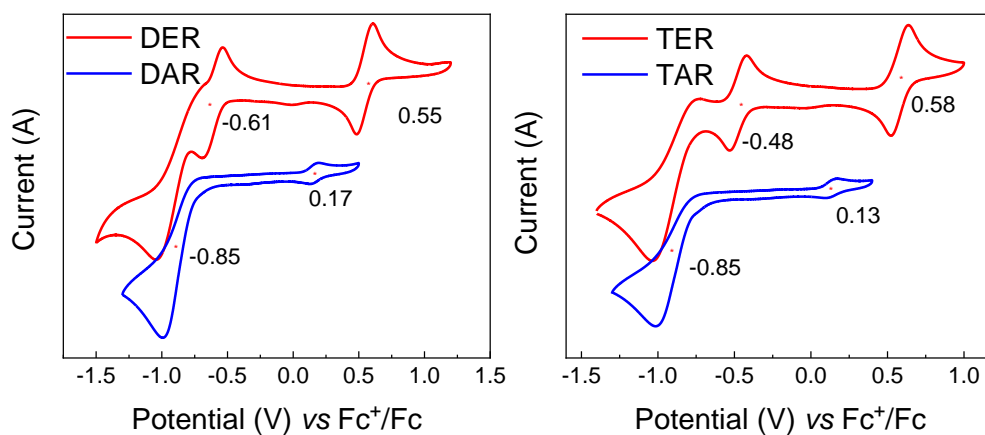
## 2.5 Absorption spectra and cyclic voltammetry

The normalized absorption spectra of these radicals displayed an intense absorption band at near 290 nm, along with weak absorption at near-ultraviolet and visible light regions.



**Figure S28.** Normalized UV absorption spectra of radicals in dichloromethane (DCM).

The CV spectra of **DER**, **TER**, **DAR** and **TAR** showed one reversible oxidation wave at  $E^{\text{OX}}_{1/2} = 0.55$  V,  $0.58$  V,  $0.17$  V,  $0.13$  V and one reduction wave at  $E^{\text{red}}_{1/2} = -0.61$  V,  $-0.48$  V,  $-0.85$  V,  $-0.85$  V, respectively. Highest occupied molecular orbital (HOMO) and lowest unoccupied molecular orbital (LUMO) energy levels were calculated to be  $-4.81$  and  $-3.65$  eV for **DER**,  $-4.84$  and  $-3.78$  eV for **TER**,  $-4.46$  and  $-3.44$  eV for **DAR**,  $-4.42$  and  $-3.44$  eV for **TAR**.

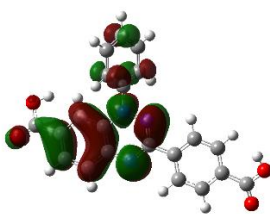
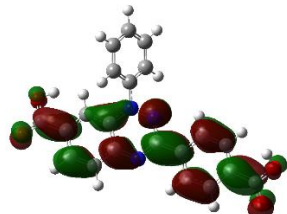
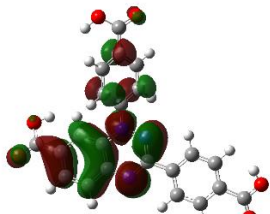
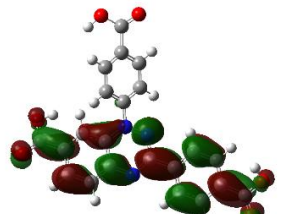


**Figure S29.** Cyclic voltammograms of radicals in dry DCM with  $0.1\text{M}$   $\text{Bu}_4\text{NPF}_6$  as the supporting electrolyte,  $\text{Ag}/\text{AgCl}$  as the reference electrode, glassy carbon as the working electrode, Pt wire as the counter electrode, and a scan rate of  $100\text{ mV s}^{-1}$ . The red stars indicate the half-wave potential  $E_{1/2}$ .

## 2.6 Gaussian simulation calculation

All calculations were performed with the Gaussian 16 program suite.<sup>[1]</sup> Full geometry optimizations were carried out at the (U)B3LYP/6–31G(d) level. The HOMO orbit was delocalized mainly on the backbone of benzotriazinyl moiety and the phenyl at N<sub>1</sub>, and the LUMO orbit was delocalized mainly on the backbone of benzotriazinyl moiety and the phenyl at N<sub>2</sub>. HOMO, LUMO and spin densities were illustrated using GaussianView 5.0.

**Table S1.** Calculated HOMO and LUMO orbits of **DAR** and **TAR**.

	HOMO <sup>α</sup>	LUMO <sup>α</sup>
DAR		
TAR		

## 2.7. ESR spectra/simulation and data analysis

Simulations of solution ESR spectra were performed with the *Easyspin* program in Matlab.<sup>[2]</sup>

ESR spectra of **DER** and **TER** in DCM and **DAR** and **TAR** in DMF at room temperature show typical seven-line patterns consistent with the coupling of the unpaired electron with three chemically distinct nitrogen atoms of the triazinyl ring.

The hyperfine coupling constants (hfcc) obtained from simulated ESR spectra are  $\alpha(\text{N1}) = 7.81$ ,  $\alpha(\text{N2}) = 4.78$ , and  $\alpha(\text{N3}) = 4.49$  G for **DER**,  $\alpha(\text{N1}) = 7.85$ ,  $\alpha(\text{N2}) = 4.67$ , and  $\alpha(\text{N3}) = 4.67$  G for **DAR**;  $\alpha(\text{N1}) = 7.39$ ,  $\alpha(\text{N2}) = 4.65$ , and  $\alpha(\text{N3}) = 4.60$  G for **TER**,  $\alpha(\text{N1}) = 7.58$ ,  $\alpha(\text{N2}) = 4.71$ , and  $\alpha(\text{N3}) = 4.61$  G for **TAR**. Spin density ( $\rho$ ) distributions were estimated from hyperfine splitting constants using McConnell's equation.

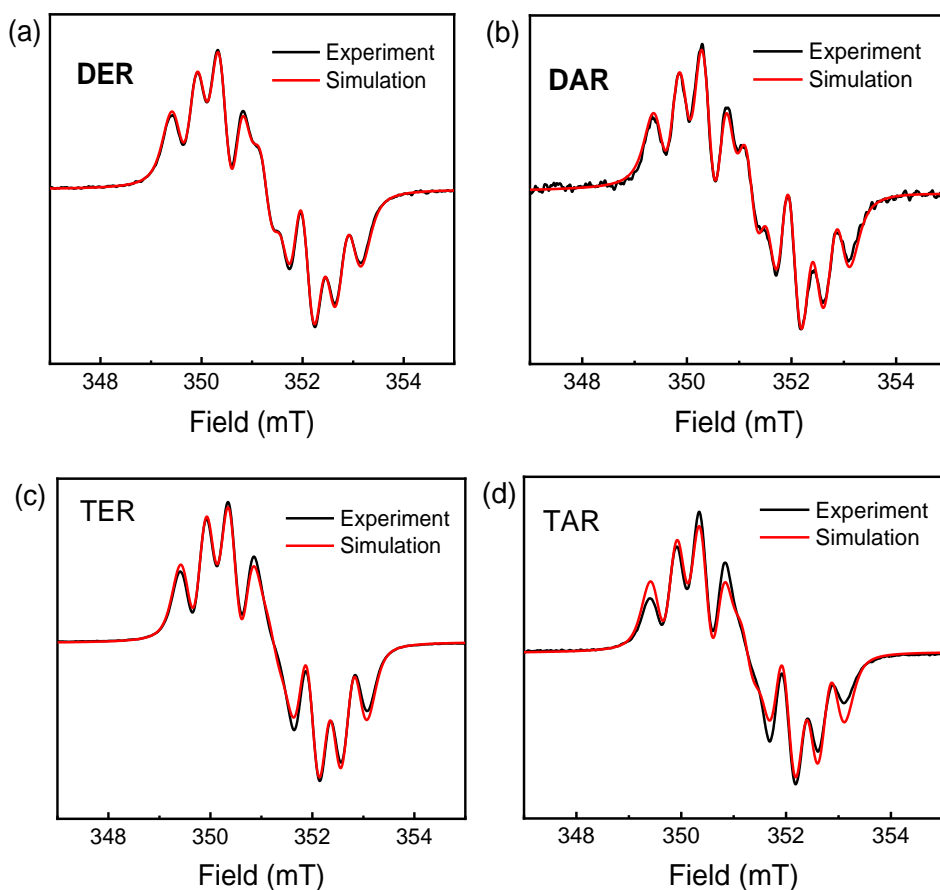


**Figure S30.** ESR spectra of **DER** (a) and **TER** (c) in DCM, **DAR** (b) and **TAR** (d) in DMF at room temperature. The black and red lines indicate experimental, simulated spectra, respectively.



**Table S2.** The hyperfine coupling constant (hfcc)  $\alpha_N$  (G) and spin densities ( $\rho_N$ ) estimated from hfcc using McConnell's equation<sup>a</sup> of **DER**, **DAR**, **TER** and **TAR**.

Compound	$\alpha_{N1}/G$	$\alpha_{N2}/G$	$\alpha_{N3}/G$	$\rho_{N1}$	$\rho_{N2}$	$\rho_{N3}$
<b>DER</b>	7.81	4.78	4.49	0.312	0.225	0.212
<b>DAR</b>	7.85	4.67	4.67	0.314	0.220	0.220
<b>TER</b>	7.39	4.65	4.60	0.296	0.219	0.217
<b>TAR</b>	7.58	4.71	4.61	0.303	0.222	0.217

<sup>a</sup>  $\alpha_N = Q_N \rho_N$ , where  $\alpha_N$  are the hfcc in Gauss;  $Q_N = 21.2$  G (for N2 and N3) and  $Q_N = 25$  G (for N1).

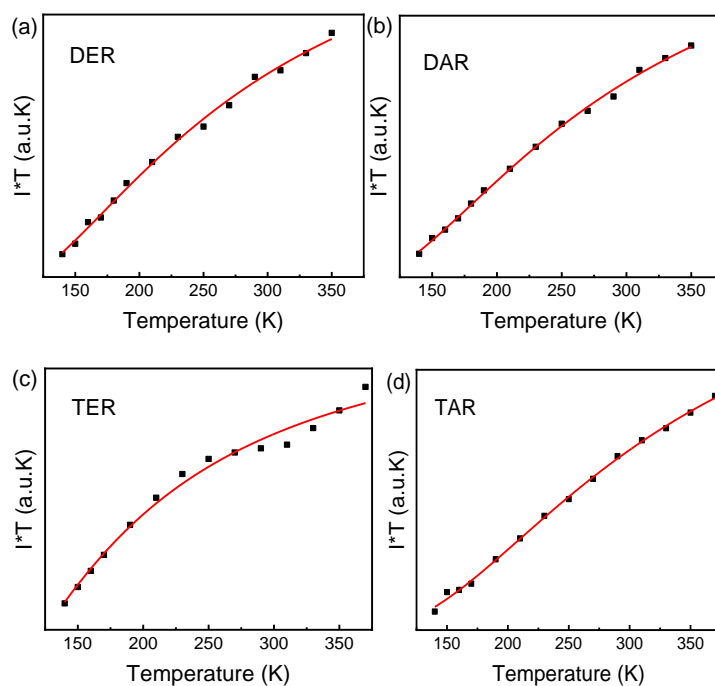


**Figure S31.** The measured (black square) and fitted (solid red line) IT-T curves of solid **DER** (a), **DAR** (b), **TER** (c) and **TAR** (d) based on the variable temperature ESR measurements from 140 to 370 K. The solid lines are the fitting curves according to Bleaney–Bowers equation; g-factor was taken to be 2.

### Data analysis

The values of singlet and triplet energy gap  $\Delta E_{S-T}$  were roughly estimated to be -0.97, -1.01, -0.64 and -1.18 kcal mol<sup>-1</sup> for **DER**, **DAR**, **TER**, **TAR** respectively. Forbidden

transition signals  $\Delta m_s = \pm 2$  was observed for **DER** (Figure S32 a).

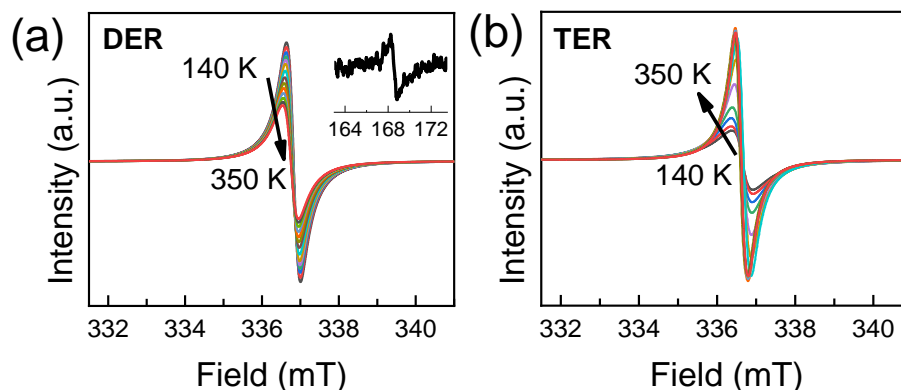


**Figure S32.** Variable temperature ESR spectra of solid **DER** (a), **TER** (b). Inset shows the half field forbidden transition signal at 140 K.

## 2.8 Magnetization measurements and data analysis

For SQUID measurements, magnetic susceptibility of powder samples of **DER** (11.9 mg), **DAR** (14.0 mg), **UD-Zn** (12.2 mg), **TER** (12.8 mg), **TAR** (11.9 mg) and **UT-Zn** (7.0 mg), was measured in a polycarbonate capsule fitted in a brass straw as a function of temperature in heating (5 K  $\rightarrow$  300 K, 3 K increase in a range 5-50 K, 4 K increase in a range 50-90 K, 15 K increase in a range 90-300 K.) at 1.0 T using a SQUID magnetometer. The data were corrected for both sample diamagnetism (Pascal's constants) and the diamagnetism of the sample holder (polycarbonate capsule) (Figure S33).

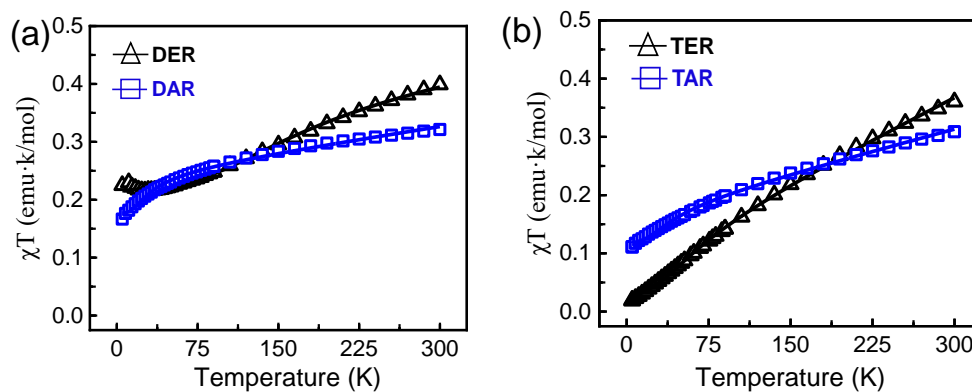


**Figure S33.** Temperature-dependent plots of  $\chi T$  measured at 1.0 T in the stable mode from 5 to 300 K. (a) **DER** (black triangle), **DAR** (blue square); (b) **TER** (black triangle), **TAR** (blue square). The solid lines are the fitting curves according to Bleaney-Bowers equation; g-factor was taken to be 2.

### Data analysis

The SQUID data were roughly fitted with a modified Bleaney-Bowers equation.

$$\chi = \frac{Ng^2\mu_B^2}{kT} \left[ \frac{2}{3 + e^{-2J/kT}} \right] (1 - \rho) + \frac{Ng^2\mu_B^2}{2kT} \rho + TIP(1 - \rho) \quad \text{Equation S1}$$

Where  $\rho$  is the fraction of  $s=1/2$  impurity,  $TIP$  is the temperature independent paramagnetism due to a small energy gap between group singlet state and excited triplet state

The estimated  $2J = -0.72$  kcal/mol for **DER**, with  $\rho = 52.8\%$ ,  $TIP = 0.4 \times 10^{-3}$  emu/mol, the Adj. R-Square  $>0.995$ .

The estimated  $2J = -0.12$  kcal/mol for **DAR**, with  $\rho = 71.7\%$ ,  $TIP = 1.0 \times 10^{-3}$  emu/mol, the Adj. R-Square  $>0.994$ .

The estimated  $2J = -0.25$  kcal/mol for **TER**, with  $\rho = 38.2\%$ ,  $TIP = 1.5 \times 10^{-3}$  emu/mol, the Adj. R-Square  $>0.998$ .

The estimated  $2J = -0.11$  kcal/mol for **TAR**, with  $\rho = 81.1\%$ ,  $TIP = 2.6 \times 10^{-3}$  emu/mol, the Adj. R-Square  $>0.997$ .

### 3. Preparation and characterization of CPs

#### 3.1 Ultrasonic synthesis:

CPs were prepared according to modified synthesis method reported by Farrukh Israr et al.<sup>[4]</sup> A solid mixture of 50  $\mu\text{mol}$  ligand **DAR** and identical metal acetate ( $\text{Cu}(\text{CH}_3\text{COO})_2 \cdot \text{H}_2\text{O}$  or  $\text{Zn}(\text{CH}_3\text{COO})_2 \cdot 2\text{H}_2\text{O}$ ) were dissolved in 4 mL N,N-diethylformamide (DEF). The formed precipitate was centrifuged and filtered upon ultrasonic irradiation for 30 min at the frequency of 40 kHz at  $0^\circ\text{C}$ . Then the resulting CPs **UD-Cu** and **UD-Zn** were solvent exchanged with DEF ( $3 \times 10$  mL) and DCM ( $3 \times 10$  mL), respectively, followed by vacuum drying at  $60^\circ\text{C}$  for 24 h. **UT-Cu** and **UT-Zn** were prepared in a similar manner by 50  $\mu\text{mol}$  ligand **TAR** and 100  $\mu\text{mol}$  metal acetate ( $\text{Cu}(\text{CH}_3\text{COO})_2 \cdot \text{H}_2\text{O}$  or  $\text{Zn}(\text{CH}_3\text{COO})_2 \cdot 2\text{H}_2\text{O}$ ). The  $\Delta E_{S-T}$  values were estimated to be  $-1.18$  and  $-0.64$  kcal  $\text{mol}^{-1}$  for **UD-Zn** and **UT-Zn**, respectively.

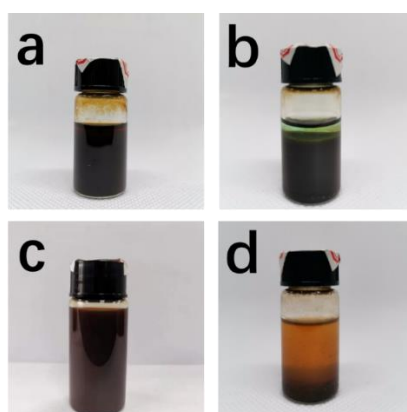


**Figure S34.** Images of ultrasonic treated solution of ligands and metal acetates for 30 mins at  $0^\circ\text{C}$ , **UD-Cu** (a), **UT-Cu** (b), **UD-Zn** (c), **UT-Zn** (d).

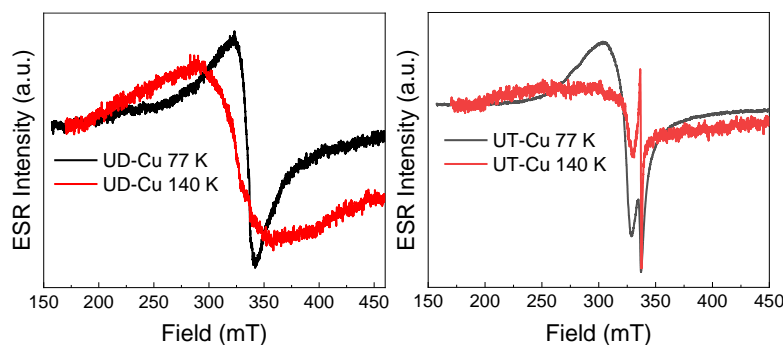


**Figure S35.** EPR spectra of **UD-Cu**, and **UT-Cu** at 77 and 140 K.

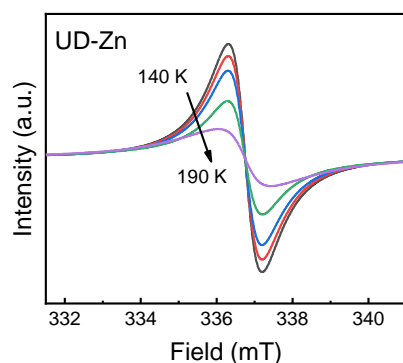


**Figure S36.** Variable temperature ESR spectra of ICP **UD-Zn** from 140 to 190 K.

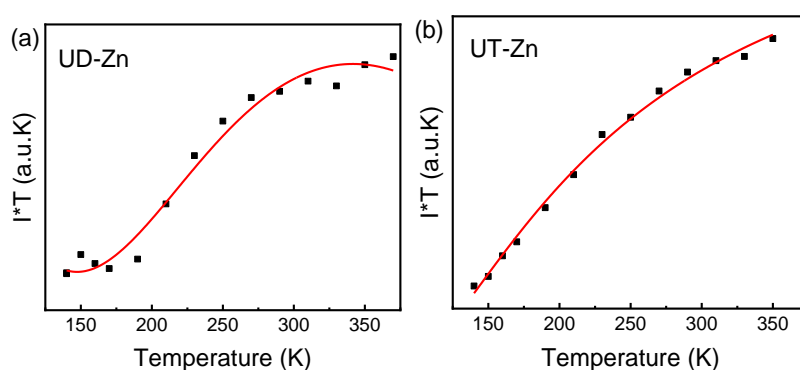


**Figure S37.** The measured (black square) and fitted (solid red line) IT-T curves of CPs **UD-Zn** (a), **UT-Zn** (b) based on the variable temperature ESR measurements from 140 to 370 K. The solid lines are the fitting curves according to Bleaney–Bowers equation; g-factor was taken to be 2.

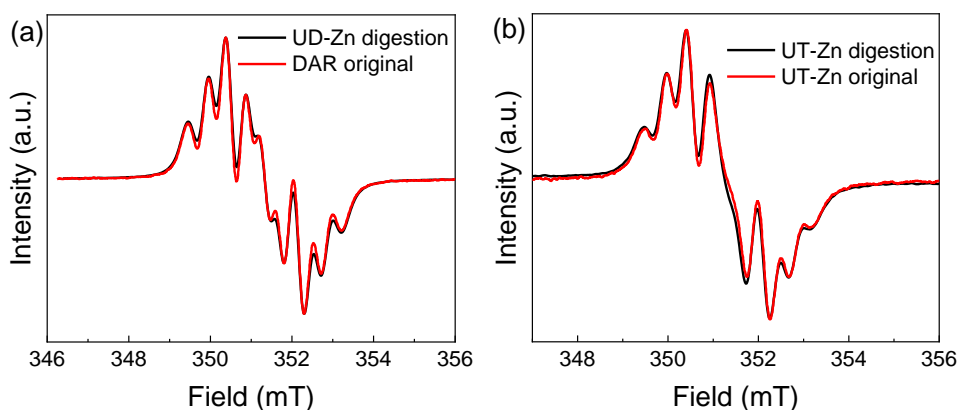


**Figure S38.** Normalized EPR spectra of **DAR** and acid digested **UD-Zn** (a), **TAR** and acid digested **UT-Zn** (b) in DEF at room temperature.

### 3.3 X-ray photoelectron spectroscopy (XPS)

For XPS measurements, the auger electron spectra were also used to accurately explain the chemical state of elements. As shown in **Figure S39 a-b**, the peaks at around 569.5 eV are related to  $\text{Cu}^{2+}$  LMM, and the typical peaks at around 571.5 eV are corresponding to  $\text{Cu}^+$  LMM. Wide spectra of copper and carbon are also given in **Figure S39 c-f**. These results support the coexistence of two valence states of copper in CPs **UD-Cu** and **UT-Cu**.

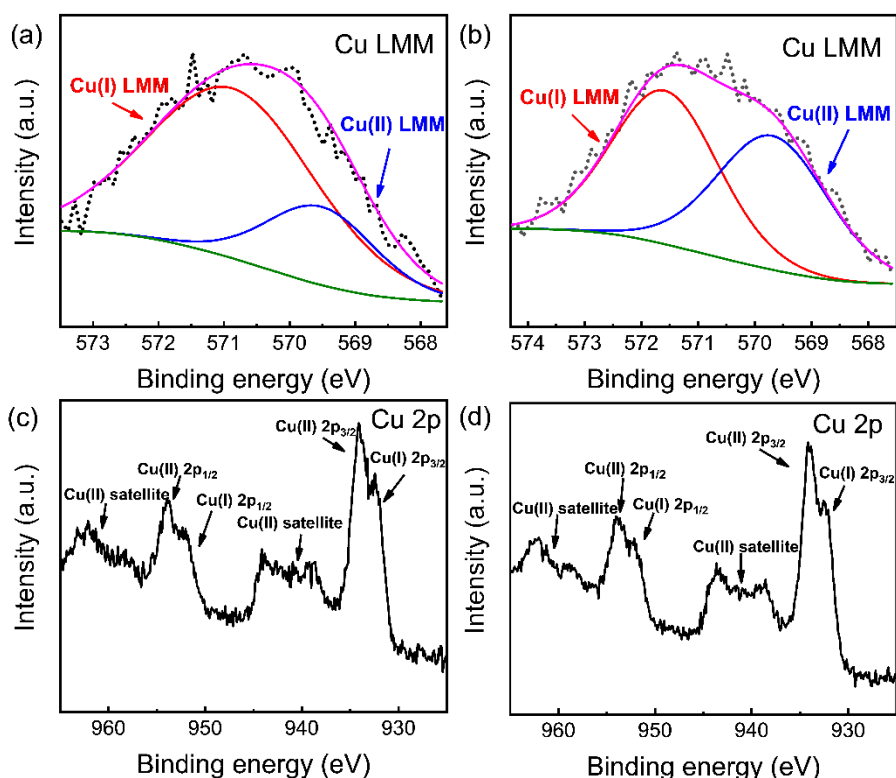


**Figure S39.** The XPS Cu auger electron spectra of **UD-Cu** (a) and **UT-Cu** (b); the Cu 2p wide spectra of **UD-Cu** (c) and **UT-Cu** (d).

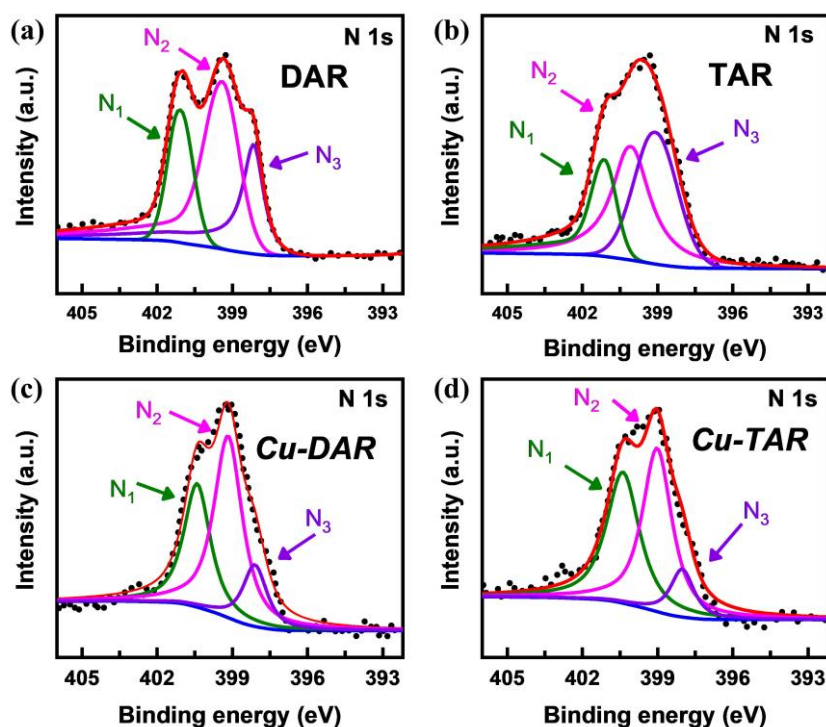


**Figure S40.** XPS spectra of N 1s on **DAR** (a), **TAR** (b), **UD-Cu** (c), and **UT-Cu** (d).

**Table S3.** ICP-MS measurements of **UD-Zn** and **UT-Zn**.

Name	Sample quality (g)	Constant volume (mL)	Dilution multiple	Zinc concentration in original solution of digestion solution ( $\mu\text{g/L}$ )	Zinc content (%)
UD-Zn	0.0153	25	1000	100114	16.36
UT-Zn	0.0195	25	1000	173618	22.26

The ratio of zinc ions to ligands was calculated to be 1:1 for **UD-Zn** and 1.5:1 for **UT-Zn** according to inductively coupled plasma mass spectrometry (ICP-MS)

## References:

- [1] M. J. Frisch GWT, H. B. Schlegel, G. E. Scuseria, ; M. A. Robb, J. R. C., G. Scalmani, V. Barone, ; G. A. Petersson, H. N., X. Li, M. Caricato, A. V. Marenich, ; J. Bloino, B. G. J., R. Gomperts, B. Mennucci, H. P. Hratchian, ; J. V. Ortiz, A. F. I., J. L. Sonnenberg, D. Williams-Young, ; F. Ding, F. L., F. Egidi, J. Goings, B. Peng, A. Petrone, ; T. Henderson, D. R., V. G. Zakrzewski, J. Gao, N. Rega, ; G. Zheng, W. L., M. Hada, M. Ehara, K. Toyota, R. Fukuda, ; J. Hasegawa, M. I., T. Nakajima, Y. Honda, O. Kitao, H. Nakai, ; T. Vreven, K. T., J. A. Montgomery, Jr., J. E. Peralta, ;

- F. Ogliaro, M. J. B., J. J. Heyd, E. N. Brothers, K. N. Kudin, ; V. N. Staroverov, T. A. K., R. Kobayashi, J. Normand, ; K. Raghavachari, A. P. R., J. C. Burant, S. S. Iyengar, ; J. Tomasi, M. C., J. M. Millam, M. Klene, C. Adamo, R. Cammi, ; J. W. Ochterski, R. L. M., K. Morokuma, O. Farkas, ; J. B. Foresman, and D. J. Fox, Gaussian 16 Revision A. 03. 2016; Gaussian Inc. Wallingford CT 2016.
- [2] Stoll,S. & Schweiger, A. *J. Magn. Reson.* **2006**, *178*, 42-55.
- [3] Xue, W. Wang, J. Huang, H. & Mei, D. *J. Phys. Chem. C.* **2021**, *125*, 5832-5847.
- [4] Farrukh, I. et al. *Ultrason. Sonochem.* **2016**, *29*, 186-193.

### Coordinates for calculated geometries:

#### DAR

Symbol	X	Y	Z
C	1.318506	4.035393	0.072724
C	0.880426	2.788049	-0.050674
C	-0.367330	2.281755	-0.069134
C	-1.173594	3.369299	0.099830
C	-0.778592	4.663708	0.131362
C	0.471533	5.014281	0.159602
N	-0.615475	0.993802	-0.092999
C	-1.726636	0.303939	-0.007356
C	-1.669939	-1.014755	0.185463
N	-0.550715	-1.635035	0.211053
C	0.546762	-1.013263	-0.010083
N	0.381445	0.222300	-0.101689
C	-3.055361	0.723820	-0.086600
C	-4.165011	-0.083449	0.106776
C	-3.942343	-1.389382	0.344218
C	-2.700286	-1.907648	0.352669
C	1.669594	-1.680327	-0.154231
C	2.842050	-1.115140	-0.331574



C	3.991874	-1.823045	-0.319222
C	4.065423	-3.153284	-0.159067
C	2.824434	-3.753164	-0.068767
C	1.660759	-3.012721	-0.070699
C	-5.359694	0.471751	0.035155
O	-6.373512	-0.171223	0.269264
O	-5.498967	1.791294	-0.237255
C	5.201172	-3.867276	-0.072851
O	5.200269	-5.083212	0.097536
O	6.379624	-3.175435	-0.142823
H	2.421827	4.075151	0.053474
H	1.763914	2.071769	-0.073780
H	-2.219580	3.127217	0.197981
H	-1.657414	5.333787	0.190683
H	0.810955	6.039780	0.222821
H	-3.231745	1.743447	-0.396729
H	-4.733893	-2.138426	0.605933
H	-2.451905	-2.946084	0.615936
H	3.006886	-0.022020	-0.504160
H	4.868655	-1.189627	-0.473075
H	2.714740	-4.836188	0.020453
H	0.768560	-3.683494	0.017924
H	-4.671271	2.277624	-0.387664
H	6.201044	-2.216063	-0.221380

## TAR

Symbol	X	Y	Z
C	0.816120	3.770110	-0.275426
C	0.716961	2.420798	-0.320024

C	-0.377848	1.769035	0.034186
C	-1.297132	2.516967	0.600144
C	-1.277677	3.865940	0.535310
C	-0.215545	4.554694	0.112872
N	-0.464461	0.507871	-0.011815
C	-1.560314	-0.164920	0.079919
C	-1.526186	-1.504887	0.147715
N	-0.402698	-2.097910	0.080634
C	0.704838	-1.488647	-0.101455
N	0.543001	-0.229598	-0.285466
C	-2.896983	0.308015	-0.080446
C	-4.047633	-0.453242	0.117116
C	-3.813579	-1.766805	0.298712
C	-2.598597	-2.344400	0.259090
C	1.815229	-2.151572	-0.293126
C	2.974449	-1.564621	-0.443160
C	4.119216	-2.271894	-0.385001
C	4.132376	-3.597179	-0.196329
C	2.908607	-4.219175	-0.078677
C	1.760290	-3.469953	-0.155543
C	-0.162360	5.883470	-0.003590
O	0.842394	6.484260	-0.396083
O	-1.320917	6.632217	0.198756
C	-5.258487	0.077340	0.013134
O	-6.231227	-0.626386	0.218167
O	-5.462366	1.376034	-0.275936
C	5.246324	-4.304467	-0.090540
O	5.242766	-5.519755	0.071087
O	6.424209	-3.603194	-0.180699
H	1.816617	4.034797	-0.659502

H	1.565949	1.854433	-0.742649
H	-2.187934	2.085665	1.100652
H	-2.157532	4.361122	0.902675
H	-3.079857	1.345783	-0.432504
H	-4.634398	-2.505351	0.489021
H	-2.415345	-3.417739	0.413539
H	3.127900	-0.479671	-0.625009
H	4.976237	-1.616319	-0.554246
H	2.785541	-5.296700	0.046862
H	0.854906	-4.114383	-0.059382
H	-2.011675	6.060519	0.605106
H	-4.619678	1.846931	-0.388614
H	6.296244	-2.636852	-0.242234